

The IceCube Neutrino Observatory

Contributions to ICRC 2015 Part I: Point Source Searches

The IceCube Collaboration

Contents

1	Results of neutrino point source searches with 2008–2014 IceCube data above 10 TeV — PoS(ICRC2015)1047	5
2	A search for neutrinos from Gamma Ray Bursts with the IceCube Neutrino Detector — PoS(ICRC2015)1048	13
3	Neutrino-triggered target-of-opportunity programs in IceCube — PoS(ICRC2015)1052	21
4	Low-energy (100 GeV – few TeV) neutrino point source searches in the southern sky with IceCube — PoS(ICRC2015)1053	29
5	Medium-energy (few TeV – 100 TeV) neutrino point source searches in the Southern sky with IceCube — PoS(ICRC2015)1056	37
6	The Online Follow-Up Framework for Neutrino Triggered Alerts from IceCube — PoS(ICRC2015)1069	45
7	Near Realtime Searches for Neutrinos from GRBs with IceCube — PoS(ICRC2015)1089	51
8	Search for neutrino emission from extended sources with the IceCube detector — PoS(ICRC2015)1091	59
9	Searching for TeV gamma-ray emission associated with IceCube high-energy neutrinos using VERITAS — PoS(ICRC2015)0785	arXiv:1509.00517
10	First combined search for neutrino point-sources in the Southern Sky with the ANTARES and IceCube neutrino telescopes — PoS(ICRC2015)1076	arXiv:1511.05025
11	Search for a correlation between the UHECRs measured by the Pierre Auger Observatory and the Telescope Array and the neutrino candidate events from IceCube — PoS(ICRC2015)1082	arXiv:1511.02109

*The 34th International Cosmic Ray Conference,
30 July- 6 August, 2015
The Hague, The Netherlands*

IceCube Collaboration Member List

M. G. Aartsen², K. Abraham³², M. Ackermann⁴⁸, J. Adams¹⁵, J. A. Aguilar¹², M. Ahlers²⁹, M. Ahrens³⁹, D. Altmann²³, T. Anderson⁴⁵, I. Ansseau¹², M. Archinger³⁰, C. Argüelles²⁹, T. C. Arlen⁴⁵, J. Auffenberg¹, X. Bai³⁷, S. W. Barwick²⁶, V. Baum³⁰, R. Bay⁷, J. J. Beatty^{17,18}, J. Becker Tjus¹⁰, K.-H. Becker⁴⁷, E. Beiser²⁹, S. BenZvi²⁹, P. Berghaus⁴⁸, D. Berley¹⁶, E. Bernardini⁴⁸, A. Bernhard³², D. Z. Besson²⁷, G. Binder^{8,7}, D. Bindig⁴⁷, M. Bissok¹, E. Blaufuss¹⁶, J. Blumenthal¹, D. J. Boersma⁴⁶, C. Boehm³⁹, M. Börner²⁰, F. Bos¹⁰, D. Bose⁴¹, S. Böser³⁰, O. Botner⁴⁶, J. Braun²⁹, L. Brayeux¹³, H.-P. Bretz⁴⁸, N. Buzinsky²², J. Casey⁵, M. Casier¹³, E. Cheung¹⁶, D. Chirkin²⁹, A. Christov²⁴, K. Clark⁴², L. Classen²³, S. Coenders³², D. F. Cowen^{45,44}, A. H. Cruz Silva⁴⁸, J. Daughhetee⁵, J. C. Davis¹⁷, M. Day²⁹, J. P. A. M. de André²¹, C. De Clercq¹³, E. del Pino Rosendo³⁰, H. Dembinski³³, S. De Ridder²⁵, P. Desiati²⁹, K. D. de Vries¹³, G. de Wasseige¹³, M. de With⁹, T. DeYoung²¹, J. C. Díaz-Vélez²⁹, V. di Lorenzo³⁰, J. P. Dumm³⁹, M. Dunkman⁴⁵, R. Eagan⁴⁵, B. Eberhardt³⁰, T. Ehrhardt³⁰, B. Eichmann¹⁰, S. Euler⁴⁶, P. A. Evenson³³, O. Fadiran²⁹, S. Fahey²⁹, A. R. Fazely⁶, A. Fedynitch¹⁰, J. Feintzeig²⁹, J. Felde¹⁶, K. Filimonov⁷, C. Finley³⁹, T. Fischer-Wasels⁴⁷, S. Flis³⁹, C.-C. Fösig³⁰, T. Fuchs²⁰, T. K. Gaisser³³, R. Gaior¹⁴, J. Gallagher²⁸, L. Gerhardt^{8,7}, K. Ghorbani²⁹, D. Gier¹, L. Gladstone²⁹, M. Glagla¹, T. Glüsenskamp⁴⁸, A. Goldschmidt⁸, G. Golup¹³, J. G. Gonzalez³³, D. Góra⁴⁸, D. Grant²², J. C. Groh⁴⁵, A. Groß³², C. Ha^{8,7}, C. Haack¹, A. Haj Ismail²⁵, A. Hallgren⁴⁶, F. Halzen²⁹, B. Hansmann¹, K. Hanson²⁹, D. Hebecker⁹, D. Heereman¹², K. Helbing⁴⁷, R. Hellauer¹⁶, D. Hellwig¹, S. Hickford⁴⁷, J. Hignight²¹, G. C. Hill², K. D. Hoffman¹⁶, R. Hoffmann⁴⁷, K. Holzapfel³², A. Homeier¹¹, K. Hoshina^{29,a}, F. Huang⁴⁵, M. Huber³², W. Huelsnitz¹⁶, P. O. Hulth³⁹, K. Hultqvist³⁹, S. In⁴¹, A. Ishihara¹⁴, E. Jacobi⁴⁸, G. S. Japaridze⁴, K. Jero²⁹, M. Jurkovic³², B. Kaminsky⁴⁸, A. Kappes²³, T. Karg⁴⁸, A. Karle²⁹, M. Kauer^{29,34}, A. Keivani⁴⁵, J. L. Kelley²⁹, J. Kemp¹, A. Kheirandish²⁹, J. Kiryluk⁴⁰, J. Kläs⁴⁷, S. R. Klein^{8,7}, G. Kohnen³¹, R. Koirala³³, H. Kolanoski⁹, R. Konietz¹, A. Koob¹, L. Köpke³⁰, C. Kopper²², S. Kopper⁴⁷, D. J. Koskinen¹⁹, M. Kowalski^{9,48}, K. Krings³², G. Kroll³⁰, M. Kroll¹⁰, J. Kunnen¹³, N. Kurahashi³⁶, T. Kuwabara¹⁴, M. Labare²⁵, J. L. Lanfranchi⁴⁵, M. J. Larson¹⁹, M. Lesiak-Bzdak⁴⁰, M. Leuermann¹, J. Leuner¹, L. Lu¹⁴, J. Lünemann¹³, J. Madsen³⁸, G. Maggi¹³, K. B. M. Mahn²¹, R. Maruyama³⁴, K. Mase¹⁴, H. S. Matis⁸, R. Maunu¹⁶, F. McNally²⁹, K. Meagher¹², M. Medici¹⁹, A. Meli²⁵, T. Menne²⁰, G. Merino²⁹, T. Meures¹², S. Miarecki^{8,7}, E. Middell⁴⁸, E. Middlemas²⁹, L. Mohrmann⁴⁸, T. Montaruli²⁴, R. Morse²⁹, R. Nahnauer⁴⁸, U. Naumann⁴⁷, G. Neer²¹, H. Niederhausen⁴⁰, S. C. Nowicki²², D. R. Nygren⁸, A. Obertacke⁴⁷, A. Olivas¹⁶, A. Omairat⁴⁷, A. O'Murchadha¹², T. Palczewski⁴³, H. Pandya³³, L. Paul¹, J. A. Pepper⁴³, C. Pérez de los Heros⁴⁶, C. Pfendner¹⁷, D. Pieloth²⁰, E. Pinat¹², J. Posselt⁴⁷, P. B. Price⁷, G. T. Przybylski⁸, J. Pütz¹, M. Quinnan⁴⁵, C. Raab¹², L. Rädcl¹, M. Rameez²⁴, K. Rawlins³, R. Reimann¹, M. Relich¹⁴, E. Resconi³², W. Rhode²⁰, M. Richman³⁶, S. Richter²⁹, B. Riedel²², S. Robertson², M. Rongen¹, C. Rott⁴¹, T. Ruhe²⁰, D. Ryckbosch²⁵, S. M. Saba¹⁰, L. Sabbatini²⁹, H.-G. Sander³⁰, A. Sandrock²⁰, J. Sandroos³⁰, S. Sarkar^{19,35}, K. Schatto³⁰, F. Scheriau²⁰, M. Schimp¹, T. Schmidt¹⁶, M. Schmitz²⁰, S. Schoenen¹, S. Schöneberg¹⁰, A. Schönwald⁴⁸, L. Schulte¹¹, D. Seckel³³, S. Seunarine³⁸, R. Shanidze⁴⁸, M. W. E. Smith⁴⁵, D. Soldin⁴⁷, M. Song¹⁶, G. M. Spiczak³⁸, C. Spiering⁴⁸, M. Stahlberg¹, M. Stamatikos^{17,b}, T. Stanev³³, N. A. Stanisha⁴⁵, A. Stasik⁴⁸, T. Stezelberger⁸, R. G. Stokstad⁸, A. Stöbl⁴⁸, R. Ström⁴⁶, N. L. Strotjohann⁴⁸, G. W. Sullivan¹⁶, M. Sutherland¹⁷, H. Taavola⁴⁶, I. Taboada⁵, S. Ter-Antonyan⁶, A. Terliuk⁴⁸, G. Tešić⁴⁵, S. Tilav³³, P. A. Toale⁴³, M. N. Tobin²⁹, S. Toscano¹³, D. Tosi²⁹, M. Tselengidou²³, A. Turcati³², E. Unger⁴⁶, M. Usner⁴⁸, S. Vallecorsa²⁴, J. Vandenbroucke²⁹, N. van Eijndhoven¹³,

S. Vanheule²⁵, J. van Santen²⁹, J. Veenkamp³², M. Vehring¹, M. Voge¹¹, M. Vraeghe²⁵, C. Walck³⁹, A. Wallace², M. Wallraff¹, N. Wandkowsky²⁹, Ch. Weaver²², C. Wendt²⁹, S. Westerhoff²⁹, B. J. Whelan², N. Whitehorn²⁹, C. Wichary¹, K. Wiebe³⁰, C. H. Wiebusch¹, L. Wille²⁹, D. R. Williams⁴³, H. Wissing¹⁶, M. Wolf³⁹, T. R. Wood²², K. Woschnagg⁷, D. L. Xu⁴³, X. W. Xu⁶, Y. Xu⁴⁰, J. P. Yanez⁴⁸, G. Yodh²⁶, S. Yoshida¹⁴, M. Zoll³⁹

¹III. Physikalisches Institut, RWTH Aachen University, D-52056 Aachen, Germany

²Department of Physics, University of Adelaide, Adelaide, 5005, Australia

³Dept. of Physics and Astronomy, University of Alaska Anchorage, 3211 Providence Dr., Anchorage, AK 99508, USA

⁴CTSPS, Clark-Atlanta University, Atlanta, GA 30314, USA

⁵School of Physics and Center for Relativistic Astrophysics, Georgia Institute of Technology, Atlanta, GA 30332, USA

⁶Dept. of Physics, Southern University, Baton Rouge, LA 70813, USA

⁷Dept. of Physics, University of California, Berkeley, CA 94720, USA

⁸Lawrence Berkeley National Laboratory, Berkeley, CA 94720, USA

⁹Institut für Physik, Humboldt-Universität zu Berlin, D-12489 Berlin, Germany

¹⁰Fakultät für Physik & Astronomie, Ruhr-Universität Bochum, D-44780 Bochum, Germany

¹¹Physikalisches Institut, Universität Bonn, Nussallee 12, D-53115 Bonn, Germany

¹²Université Libre de Bruxelles, Science Faculty CP230, B-1050 Brussels, Belgium

¹³Vrije Universiteit Brussel, Dienst ELEM, B-1050 Brussels, Belgium

¹⁴Dept. of Physics, Chiba University, Chiba 263-8522, Japan

¹⁵Dept. of Physics and Astronomy, University of Canterbury, Private Bag 4800, Christchurch, New Zealand

¹⁶Dept. of Physics, University of Maryland, College Park, MD 20742, USA

¹⁷Dept. of Physics and Center for Cosmology and Astro-Particle Physics, Ohio State University, Columbus, OH 43210, USA

¹⁸Dept. of Astronomy, Ohio State University, Columbus, OH 43210, USA

¹⁹Niels Bohr Institute, University of Copenhagen, DK-2100 Copenhagen, Denmark

²⁰Dept. of Physics, TU Dortmund University, D-44221 Dortmund, Germany

²¹Dept. of Physics and Astronomy, Michigan State University, East Lansing, MI 48824, USA

²²Dept. of Physics, University of Alberta, Edmonton, Alberta, Canada T6G 2E1

²³Erlangen Centre for Astroparticle Physics, Friedrich-Alexander-Universität Erlangen-Nürnberg, D-91058 Erlangen, Germany

²⁴Département de physique nucléaire et corpusculaire, Université de Genève, CH-1211 Genève, Switzerland

²⁵Dept. of Physics and Astronomy, University of Gent, B-9000 Gent, Belgium

²⁶Dept. of Physics and Astronomy, University of California, Irvine, CA 92697, USA

²⁷Dept. of Physics and Astronomy, University of Kansas, Lawrence, KS 66045, USA

²⁸Dept. of Astronomy, University of Wisconsin, Madison, WI 53706, USA

²⁹Dept. of Physics and Wisconsin IceCube Particle Astrophysics Center, University of Wisconsin, Madison, WI 53706, USA

³⁰Institute of Physics, University of Mainz, Staudinger Weg 7, D-55099 Mainz, Germany

- ³¹Université de Mons, 7000 Mons, Belgium
- ³²Technische Universität München, D-85748 Garching, Germany
- ³³Bartol Research Institute and Dept. of Physics and Astronomy, University of Delaware, Newark, DE 19716, USA
- ³⁴Dept. of Physics, Yale University, New Haven, CT 06520, USA
- ³⁵Dept. of Physics, University of Oxford, 1 Keble Road, Oxford OX1 3NP, UK
- ³⁶Dept. of Physics, Drexel University, 3141 Chestnut Street, Philadelphia, PA 19104, USA
- ³⁷Physics Department, South Dakota School of Mines and Technology, Rapid City, SD 57701, USA
- ³⁸Dept. of Physics, University of Wisconsin, River Falls, WI 54022, USA
- ³⁹Oskar Klein Centre and Dept. of Physics, Stockholm University, SE-10691 Stockholm, Sweden
- ⁴⁰Dept. of Physics and Astronomy, Stony Brook University, Stony Brook, NY 11794-3800, USA
- ⁴¹Dept. of Physics, Sungkyunkwan University, Suwon 440-746, Korea
- ⁴²Dept. of Physics, University of Toronto, Toronto, Ontario, Canada, M5S 1A7
- ⁴³Dept. of Physics and Astronomy, University of Alabama, Tuscaloosa, AL 35487, USA
- ⁴⁴Dept. of Astronomy and Astrophysics, Pennsylvania State University, University Park, PA 16802, USA
- ⁴⁵Dept. of Physics, Pennsylvania State University, University Park, PA 16802, USA
- ⁴⁶Dept. of Physics and Astronomy, Uppsala University, Box 516, S-75120 Uppsala, Sweden
- ⁴⁷Dept. of Physics, University of Wuppertal, D-42119 Wuppertal, Germany
- ⁴⁸DESY, D-15735 Zeuthen, Germany
- ^aEarthquake Research Institute, University of Tokyo, Bunkyo, Tokyo 113-0032, Japan
- ^bNASA Goddard Space Flight Center, Greenbelt, MD 20771, USA

Acknowledgment: We acknowledge the support from the following agencies: U.S. National Science Foundation-Office of Polar Programs, U.S. National Science Foundation-Physics Division, University of Wisconsin Alumni Research Foundation, the Grid Laboratory Of Wisconsin (GLOW) grid infrastructure at the University of Wisconsin - Madison, the Open Science Grid (OSG) grid infrastructure; U.S. Department of Energy, and National Energy Research Scientific Computing Center, the Louisiana Optical Network Initiative (LONI) grid computing resources; Natural Sciences and Engineering Research Council of Canada, WestGrid and Compute/Calcul Canada; Swedish Research Council, Swedish Polar Research Secretariat, Swedish National Infrastructure for Computing (SNIC), and Knut and Alice Wallenberg Foundation, Sweden; German Ministry for Education and Research (BMBF), Deutsche Forschungsgemeinschaft (DFG), Helmholtz Alliance for Astroparticle Physics (HAP), Research Department of Plasmas with Complex Interactions (Bochum), Germany; Fund for Scientific Research (FNRS-FWO), FWO Odysseus programme, Flanders Institute to encourage scientific and technological research in industry (IWT), Belgian Federal Science Policy Office (Belspo); University of Oxford, United Kingdom; Marsden Fund, New Zealand; Australian Research Council; Japan Society for Promotion of Science (JSPS); the Swiss National Science Foundation (SNSF), Switzerland; National Research Foundation of Korea (NRF); Danish National Research Foundation, Denmark (DNRF)

Results of neutrino point source searches with 2008-2014 IceCube data above 10 TeV

The IceCube Collaboration[†]

[†] http://icecube.wisc.edu/collaboration/authors/icrc15_icecube

E-mail: coenders@icecube.wisc.edu

The emphasis on point-like source searches for astrophysical neutrinos has recently been strengthened by the unambiguous detection of high-energy astrophysical neutrinos by IceCube. So far, the limited statistics and angular resolution of the relevant analyses do not resolve more than an isotropic emission of astrophysical neutrinos. We present the results of searches for neutrino emission of point-like sources using six years of integrated IceCube livetime, of which three years use the complete IceCube detector. Focusing on track-like events induced by charged-current muon-neutrinos, a large statistics sample of $\sim 600\,000$ events on the full sky with median angular resolution between 1° and 0.4° , improving with higher energy, has been collected. For the southern hemisphere, the main background consists of bundles of muons created in extensive air-showers in the Earth's atmosphere, whereas the northern hemisphere is dominated by neutrinos created in the same process. Using an unbinned likelihood maximization search for local clustering, IceCube is sensitive to sources in the northern sky with fluxes substantially below $E^2 \partial\phi / \partial E = 10^{-12} \text{ TeV cm}^{-2} \text{ s}^{-1}$. We report about the status of these searches and the implications on the nature of the observed flux as well as on single source candidates.

Corresponding authors: Stefan Coenders^{*1}, Elisa Resconi¹

¹*Technische Universität München, Physik-Department, Boltzmannstr. 2, 85748 Garching*

*The 34th International Cosmic Ray Conference,
30 July- 6 August, 2015
The Hague, The Netherlands*

^{*}Speaker.

1. Introduction

IceCube is a cubic-kilometer neutrino detector installed in the ice at the geographic South Pole [1] between depths of 1450 m and 2450 m. Detector construction started in 2005 and finished in 2010. Neutrino reconstruction relies on the optical detection of Cherenkov radiation emitted by secondary particles produced in neutrino interactions in the surrounding ice or the nearby bedrock. During construction, partial detector configurations were operational taking data with 40 strings from April 2008, 59 strings from May 2009, and 79 strings from May 2010 on before IceCube was fully operational in May 2011.

The observation of high-energy astrophysical neutrinos by IceCube in events starting in the detector volume [2, 3] as well as up-going muons created in charged-current muon-neutrino interactions outside the detector [4, 5] strengthens the importance of searches for point-like sources of neutrinos of astrophysical origin. Neutrinos are the ideal astrophysical messenger to study acceleration mechanisms of Cosmic Rays (CRs). In hadronic interactions, neutrinos are produced alongside photons and charged particles, but due to their neutral charge and low interaction cross-section, neutrinos are neither deflected by magnetic fields, nor absorbed by interstellar media. If hadronic processes are part of the acceleration mechanisms of cosmic rays, both gamma-rays and neutrinos are produced in the decay of neutral or charged pions, respectively. Hence, using observed gamma-ray observations, predictions about the neutrino emission can be made. Almost independent of the emission spectrum of neutrinos at the source, neutrino oscillations will convert a significant amount (approximately 1/3) of the flux into $\nu_\mu + \bar{\nu}_\mu$ events that produce track-like signatures in IceCube. The first detection of a cosmic neutrino point-like source will represent a major breakthrough and will provide unique insights into aspects of cosmic ray sources.

Presently, the astrophysical signal is compatible with an isotropic distribution, which might be because of the low statistics and large angular uncertainties in the case of events starting in the detector [2], or vast atmospheric backgrounds for through-going muon searches [4, 5, 6, 7]. In order to study in more detail this new neutrino signal, dedicated point-like source searches are performed. Muons induced by high energy ν_μ penetrate through several kilometers in the Antarctic ice and hence IceCube collects muons from an effective volume much larger than the instrumented volume. Although the energy information on these through-going events is only a lower bound on the original neutrino energy, their high statistics and excellent angular uncertainty render them ideal candidates for the search for point-like sources of neutrino emission.

The main background for the search of steady neutrino sources comes from neutrinos and muons produced in the atmosphere by extensive air showers. Integrating over long enough time, a steady neutrino source will reveal itself by an increasing excess of events around the source direction over an isotropic background. Furthermore, source models and the observed astrophysical neutrino signal predict a hard energy spectrum for neutrino production at the source ($\sim E^{-2}$), whereas the atmospheric background follows a much softer spectrum ($\sim E^{-3.7}$).

We present here results from an unbiased all-sky scan and the search for neutrino emission from a limited list of known non-thermal objects. The analyses presented are based on a sample integrated over a livetime of 2063 days. This yields an event sample of approximately 600 000 events, providing the currently best neutrino point-like source sensitivity at energies above 100 TeV.

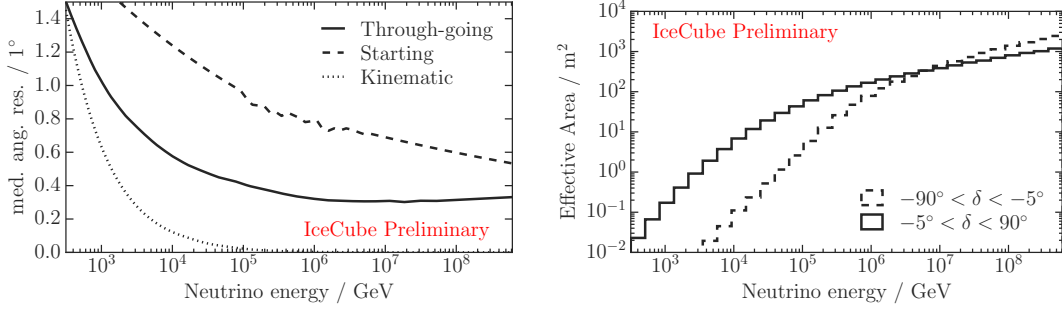


Figure 1: Angular uncertainty (left) and effective area (right) of the IceCube through-going muon point-like source analysis. The left plot also shows the intrinsic directional uncertainty due to the kinematic angle between the muon and primary neutrino. Reconstruction resolution is shown for two event topologies, namely through-going muons and muons that start within the detector. The effective area is shown for up- (solid) and down-going (dashed) events separately.

2. Detector Performance

The searches for point-like neutrino sources presented here are performed on a sample of through-going muons. At high energies, the muon direction is well correlated with the primary muon-neutrino direction, and the muon itself is reconstructed with an angular uncertainty well below 1° . The median angular resolution is shown in Fig. 1, displaying both the kinematic limit of the neutrino interaction and the reconstruction accuracy of the muon direction with respect to the neutrino direction versus the reconstructed neutrino energy. Increasing with energy, more light is deposited in the detector, giving more information about the event and thus allowing for a better reconstruction.

The event selection techniques applied here are described in [6, 7] in detail. After triggering, the over-all background rate is reduced by applying cuts on the quality of the track reconstruction against misreconstructed events. In the atmospheric muon dominated southern hemisphere (down-going), an additional charge threshold of 1 000 photoelectrons (p.e.) is applied to reduce the event rate to the level of the other hemisphere. Subsequently, multivariate selection criteria are applied in order to select well reconstructed muons which carry the most relevant information for point-like source searches; the selection is split for the two hemispheres, taking into account the different backgrounds present there. The selection for each hemisphere is discussed in the following paragraphs.

In the northern hemisphere and the region up to 5° above the horizon (*up-going* neutrinos), a pure sample of muon-neutrino induced track-like events is selected using Boosted Decision Tree (BDT) techniques. The surrounding ice and Earth matter shield IceCube from atmospheric muon events; up-going muons can only be a result of a prior charged-current neutrino interaction. Nevertheless, the main background consists of muons that enter from above but are falsely reconstructed as up-going in the detector. A second background for the search of astrophysical sources consists of atmospheric neutrinos that are created in decays of charged π^\pm and K^\pm . Atmospheric neutrinos form an irreducible component of the background and can only be disentangled statistically from the signal of high-energy astrophysical neutrinos, because atmospheric events follow a softer

spectrum than the expected signal. The background of misreconstructed muons can effectively be removed by BDTs using reconstruction quality parameters. The multivariate classification is trained using experimental data as background, which is dominated by misreconstructed muons, and Monte Carlo simulation of muon neutrinos that interact via charged-current and are reconstructed to within 3° with respect to the primary neutrino. Two BDTs are trained using different power-law energy spectra E^{-2} and $E^{-2.7}$ benchmarking extra-galactic and galactic scenarios, respectively. Using eleven variables connected to track-quality, event topology, and event-quality, effectively all muons can be rejected as misreconstructed. The final cut on the BDT score is optimized to give the best discovery potential for both hard extra- (E^{-2}) and softer galactic ($E^{-2.7}$) energy spectra.

In the southern hemisphere, the picture is different, which is why an independent selection is performed: Following the primary cosmic-ray energy spectrum, the muon rate falls more rapidly with energy than the expected high energy astrophysical neutrino flux. Consequently, the signal to background rate improves with energy. However, cosmic ray induced air showers produce bundles of muons with high multiplicity. In the detector, this deposits large amounts of energy, faking a single high-energy muon signature. Nevertheless, in contrast to single muons, a bundle produces light by superposition of many Cherenkov-cones washing out the photon arrival times at IceCube's optical sensors (Digital Optical Modules, DOMs). Besides, the energy deposition is smooth over the track distance, whereas a single high-energy muon loses energy via radiative losses showing a large stochasticity along the track. Utilizing this information of photon arrival times with respect to that of a single muon and the differential energy depositions along the track, IceCube has some power to distinguish the signal of single muons at high energies from bundles of atmospheric muons. In the BDT training procedure this is utilized using four different variables, two for the arrival times, and two for the energy depositions. Eight additional variables are chosen to select events that show the best reconstruction and event quality for point-like source related searches. Due to the vast background, the energy-threshold in the down-going region is very high, and only one BDT is trained for hard spectra (E^{-2}).

In addition to through-going muon events at very high energies, events starting in IceCube can be used to provide additional sensitivity towards point-like sources at lower energies. This is achieved using an active veto of the outer layer of DOMs as described in [2]. Most of the atmospheric muons can be identified as entering IceCube from outside and are thereby rejected, as well as atmospheric neutrinos that are accompanied by muons created in the development of the same shower [8]. In contrast to diffuse searches [2, 3], point-like source searches can allow more background because the expected signal is clustering on small scales (below 1°), whereas the background is distributed over the entire sky. Moreover, a large off-source region can be used to constrain the background using a data-driven approach. Thus, using a charge threshold of 1500 p.e. for track-like events, 549 starting events are observed within 988 days. These events have a higher probability to be of astrophysical origin than through-going events because the background rate is significantly reduced by using the veto. However, due to a smaller lever arm, the uncertainty of the reconstructed direction is worse than for through-going events as shown in Fig. 1.

Using the selection described above, the final sample consists of an almost pure muon neutrino sample at 2.4 mHz in the northern hemisphere (up-going). For the southern hemisphere, the final rate is 1.1 mHz which is about half of that in previous years. The difference is due to the starting

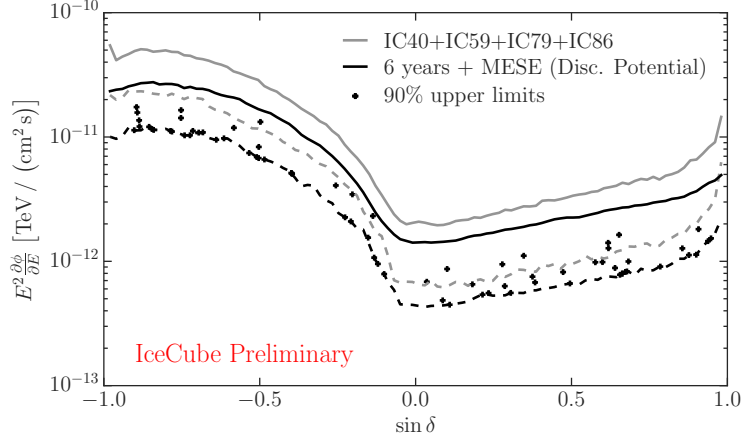


Figure 2: IceCube sensitivity (dashed) and discovery potential (solid) for steady point-like sources using six years of accumulated data. This analysis (black) adds two years to the previous analysis [7] (gray). Black crossed indicate 90% upper limits for selected source candidates at their declinations.

event sample which is more efficient at lower energies. In total, 600585 events are recorded over the full sky within 2063 days of livetime.

3. Method

The sky is probed for local clustering using an unbinned likelihood maximization

$$L = \prod_i \prod_{j \in i} \left(\frac{n_s^j}{N} S(|\mathbf{x}_j - \mathbf{x}_s|, E_j, \sigma_j; \gamma) + \left(1 - \frac{n_s^j}{N} \right) B(\delta_j, E_j) \right) \quad (3.1)$$

for all events j (total N) at location \mathbf{x}_j (declination δ_j), with energy E_j and reconstruction uncertainty σ_j , to be associated with a source at position \mathbf{x}_s and spectral index γ . The signal probability S assumes Gaussian uncertainties in the reconstruction at the source location \mathbf{x}_s . The background probability is obtained using experimental data from a large fraction of the sky as off-source region. In addition to the event position relatively to the source, energy information of each event is used to discriminate a source with hard power-law $E^{-\gamma}$ from background that is following an atmospheric spectrum. Different detector configurations (partial with respect to full operation) and event selections (starting events versus through-going) are denoted with i and their corresponding expected neutrino rates are taken into account by distributing the total number of clustered events n_s among the samples: $n_s = \sum_i n_s^i$ assuming a source with power-law spectrum $\propto E^{-\gamma}$.

The likelihood (3.1) is maximized with respect to the null hypothesis $n_s = 0$ that no significant clustering is observed. The ratio of best fit to null hypothesis forms the test statistic from which the p-value is calculated. For IceCube located at the South Pole, scrambling events in right ascension yields a perfect pure background sample that is used to construct p-values at each point.

Figure 2 shows the sensitivity and discovery potential for six years of IceCube livetime. The sensitivity is defined as the signal flux for which 90% of experiments yield a test statistics value that is equal or higher than the median value from background fluctuations only, the discovery potential

is defined as the source flux which yields a p-value at the 5σ level in 50% of the experiments. For the first time, the sensitivity surpasses $10^{-12} \text{ TeV} / \text{cm}^2 \text{ s}$ in most of the northern hemisphere assuming an unbroken E^{-2} spectrum.

3.1 All Sky Scan

Using events distributed over the entire sky, the full sky except for a small region 5° around the poles is scanned for possible clustering. The likelihood (3.1) is maximized for the number of events n_s associated to the point that is probed, as well as the spectral index γ of the source. The grid used for scanning the sky is chosen to match the typical resolution, using 0.5° spacing at the equator. The most interesting points (*hotspots*) are followed up with a finer scan using a width below 0.1° .

For each hemisphere, the most significant spot on the sky is selected according to its p-value using the test-statistic distribution of background scrambled skymaps. Those *hotspots* are trial corrected by repeating this procedure on the entire sky for pure background samples.

3.2 A Priori Source list

In addition to a full sky scan, two source lists of interesting non-thermal candidates were chosen *a-priori* containing promising candidates for neutrino emission at high energies. The candidates are known by gamma-ray observations and fall into various categories, including galactic sources like pulsar wind nebulae, supernovae remnants, etc., or extra-galactic components as BL Lacs, FSRQs, etc. Both source lists contain less than 50 sources. Consequently, the trial factor is significantly reduced compared to the full sky search, which approximately consists of 100 000 to 120 000 independent points per hemisphere.

The first source list is similar to the one used in [6, 7], setting the focus on the northern hemisphere where IceCube is most-sensitive over a wide-energy range, while only the most promising sources in the southern hemisphere are included as the energy threshold is higher. The source list contains 44 sources, of which 14 are of galactic origin.

The second source list consists of 31 sources in the southern hemisphere, the major part (21) being galactic. This list includes sources that are expected to have softer energy spectra than those in the first list. For these starting events (with their superior background suppression) are better suited than through-going muons. Using the starting event approach based on the veto technique used in [2], the energy threshold can be lowered to 100 TeV. With different techniques [9, 10], IceCube can reach lower energies in the southern hemisphere.

For both lists, the most interesting source is trial corrected using background scrambled datasets to obtain the post-trial p-value. This is done for northern and southern sources separately. Hence, three p-values are calculated from the individual source lists.

4. Results

In the analysis of six years through-going track data of the IceCube neutrino observatory, no clustering significantly above background expectation was found. Both the most interesting points in the all-sky search as well as the gamma-ray source list are compatible with background expectation.

Table 1: Selected source candidates of the two *a-priori* lists. Listed are the post-trial p-value, the fit result of the unbinned likelihood, and an upper limit on an unbroken E^{-2} spectrum $\phi_{\nu_\mu+\bar{\nu}_\mu}^{90\%}$ in units of $\text{TeV} / \text{cm}^2 \text{ s}$. Post-trial p-Values are quoted only for the most significant sources per list and hemisphere.

Source	n_s	p-Value	$\phi_{\nu_\mu+\bar{\nu}_\mu}^{90\%}$
Cygnus A	4.0	0.89	1.63
PKS 1406-076	12.9	0.051	2.32
PKS 0727-11	6.6	0.64	3.46
Mrk 421	5.5	—	1.27
Crab Nebula	6.8	—	0.75

In the northern hemisphere, the most significant spot is located at $\alpha = 249.6^\circ$, $\delta = 63.6^\circ$. The best fitting parameters at this point yield $n_s = 29$ and $\gamma = 2.1$ with a pre-trial p-Value of $-\log_{10} p = 5.75$. After trial-correction, the post-trial p-Value equals 35%. In the southern hemisphere, the best fitting point of $n_s = 19$, $\gamma = 2.3$ is located at $\alpha = 300.4^\circ$, $\delta = -33.2^\circ$. The corresponding pre-trial p-Value of 4.74 results in a trial corrected post-trial p-Value of 87%, that is, well compatible with background expectation.

Regarding the two *a priori* source lists, all outcomes can be explained with a pure background scenario as well. The most interesting candidate, the FSRQ PKS 1406-076, has a post-trial p-Value of 5.1%. This source is part of the southern part of the first source list used in this analysis. The most interesting sources are listed in Tab. 1.

5. Sensitivity to Neutrino point-like source Models

In addition to probing every point in the sky for clustering of neutrinos, neutrinos and gamma-rays can be correlated by hadronic interactions in the acceleration of cosmic rays. Here, we discuss two promising sources: the Crab nebula as the most powerful TeV gamma-ray source in the sky, and Mrk421, the closest Blazar as extra-galactic source. Model predictions connect the observed gamma-ray spectrum [11] or use Monte Carlo simulation of inelastic proton scattering at the source [12] to make predictions about the neutrino spectrum. IceCube observes small clustering at the position of the Crab nebula (Tab. 1, $\delta = 22.01^\circ$, $\alpha = 83.63^\circ$), resulting in a 90% upper limit above the sensitivity. In the case of [11], IceCube's limit is 30% above the predicted flux, whereas the limits of IceCube constrain the harder flux of [12]. Figure 3 (left) shows the upper limits of IceCube for the predictions of neutrino emission at the position of the Crab nebula.

For Mrk421, the authors of [13] derive a neutrino spectrum based on a fit to the multiwavelength photon spectrum of the source. At the location of Mrk421 ($\delta = 38.21^\circ$, $\alpha = 166.11^\circ$) IceCube's upper limit surpasses this model prediction by 16% (Fig. 3).

6. Conclusion

After starting full operation in May 2011, three years of data using the full 86-string detector have been used in the search for steady point sources. This is supplemented by three years of data with the detector in partial configuration, adding up to a total of 2063 days of detector livetime and 600585 events.

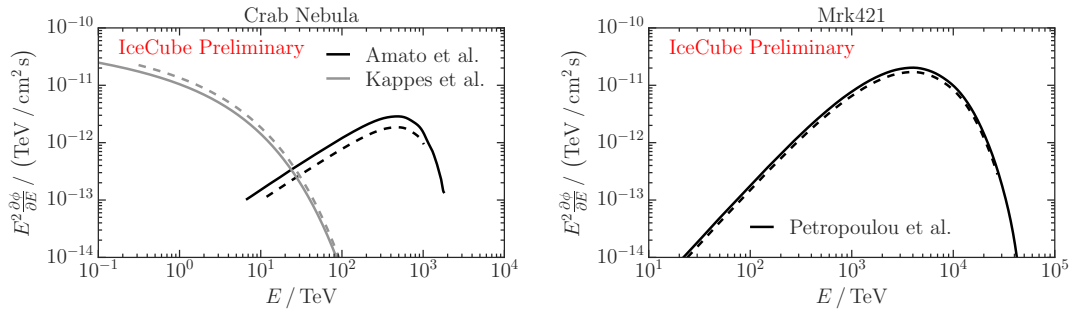


Figure 3: Model predictions of muon neutrino fluxes for the Crab nebula (PWN) [11, 12], and the BL Lac Mrk421 [13], both located in the northern hemisphere where IceCube is most sensitive. Solid lines indicate the model prediction, dashed lines the 90% upper limit with respect to the model.

In the analysis of the full sky and selected source lists, all results are consistent with pure background expectation. The most significant source PKS 1406-076 is connected to an over-fluctuation at a p-Value of 5.1%. With the obtained sensitivity, IceCube can put stringent upper limits on model predictions for the Crab nebula and Mrk421. So far, IceCube’s sensitivity is the best for neutrino point-like source emission in the TeV-PeV, and in the PeV-EeV in the northern-, southern sky, respectively. For the first time, the northern sky sensitivity reaches below $10^{-12} \text{ TeV cm}^{-2} \text{ s}^{-1}$ over most of the declination range of IceCube.

References

- [1] **IceCube** Collaboration, A. Achterberg et al., *Astropart.Phys.* **26** (2006) 155–173, [[astro-ph/0604450](#)].
- [2] **IceCube** Collaboration, M. Aartsen et al., *Phys.Rev.Lett.* **113** (2014) 101101, [[arXiv:1405.5303](#)].
- [3] **IceCube** Collaboration, M. Aartsen et al., *Phys.Rev.* **D91** (2015), no. 2 022001, [[arXiv:1410.1749](#)].
- [4] **IceCube** Collaboration, M. G. Aartsen et al., [[arXiv:1507.04005](#)].
- [5] **IceCube** Collaboration, *POS(ICRC2015)1079 these proceedings* (2015).
- [6] **IceCube** Collaboration, M. Aartsen et al., *Astrophys.J.* **779** (2013) 132, [[arXiv:1307.6669](#)].
- [7] **IceCube** Collaboration, M. Aartsen et al., [[arXiv:1406.6757](#)].
- [8] T. K. Gaisser, K. Jero, A. Karle, and J. van Santen, *Phys.Rev.* **D90** (2014), no. 2 023009, [[arXiv:1405.0525](#)].
- [9] **IceCube** Collaboration, *PoS(ICRC2015)1053 these proceedings* (2015).
- [10] **IceCube** Collaboration, *PoS(ICRC2015)1056 these proceedings* (2015).
- [11] A. Kappes et al., *The Astrophysical Journal* **656** (2007), no. 2 870.
- [12] E. Amato, D. Guetta, and P. Blasi, *Astron.Astrophys.* **402** (2003) 827–836, [[astro-ph/0302121](#)].
- [13] M. Petropoulou et al., *Mon.Not.Roy.Astron.Soc.* **448** (2015), no. 4 3121–3131, [[arXiv:1501.07407](#)].

A search for neutrinos from Gamma Ray Bursts with the IceCube Neutrino Detector

The IceCube Collaboration¹

¹http://icecube.wisc.edu/collaboration/authors/icrc15_icecube

E-mail: martin.casier@vub.ac.be

The origin of the Ultra-High Energy Cosmic Rays (UHECRs) is still unknown. Gamma-Ray Bursts (GRBs) are generally presented as possible candidates to host progenitors producing such UHECRs. However, the exact physical processes underlying GRBs are yet not fully understood. If GRBs are (partly) responsible for the observed UHECRs, they have to contain a hadronic component, and consequently high-energy neutrinos must also be produced. In this case, large scale neutrino observatories on Earth, such as the cubic kilometer IceCube Neutrino Observatory located at the South Pole, should be able to detect them. We present a new search method based on two separate datasets: the long ($T_{90} > 2\text{ s}$) and short ($T_{90} \leq 2\text{ s}$) GRBs. They will be treated separately in order to obtain the best possible sensitivity as the commonly accepted picture is that long GRBs and short GRBs have a different progenitor. Our studies will be based on different event selections and specific statistical methods.

Corresponding authors: L. Brayeur*, M. Casier*, G. Golup and N. van Eijndhoven

Vrije Universiteit Brussel, Dienst ELEM

Pleinlaan 2, B-1050 Brussels, Belgium

*The 34th International Cosmic Ray Conference,
30 July- 6 August, 2015
The Hague, The Netherlands*

*Speaker.

1. Introduction

Cosmic rays are observed in a very broad range of energies, up to about 10^{20} eV and the origin of the highest energy part is still puzzling. Gamma-ray bursts (GRBs) have been proposed [1, 2] as promising candidates to host progenitors producing the Ultra-High Energy Cosmic Rays (UHECRs) because of their extremely large energy release (of the order of $\sim 10^{54} \times \frac{\Omega_\gamma}{4\pi} \sim 10^{51}$ ergs, where Ω_γ is the solid angle into which the gamma-rays are beamed) over time scales of only $\sim 10^{-3} - 10^3$ s. In this context, a mechanism for particle acceleration during these cataclysmic events has been developed [3, 4, 5]. It is known as the *fireball model*, in which gamma-rays are produced by the dissipation of kinetic energy in an ultra-relativistic fireball. If GRBs accelerate protons through sufficiently efficient processes, they could account for most or all of the UHECR flux [2]. In this case, a neutrino signal is also expected because the accelerated protons and ambient photons will interact through the Δ -resonance and produce charged pions : $p + \gamma \rightarrow \Delta^+ \rightarrow n + \pi^+$. These charged pions will then decay leptonically via $\pi^+ \rightarrow \mu^+ + \nu_\mu$ followed by $\mu^+ \rightarrow e^+ + \nu_e + \bar{\nu}_\mu$. Therefore, the fireball should result in a flux of high-energy ν_μ and ν_e , coincident with the gamma rays [6]. Such a flux should be detectable on Earth by a sufficiently large detector. Although only ν_μ and ν_e are produced at the source, on Earth the total neutrino flux is expected to be equally composed of three neutrino flavors because of neutrino oscillations. Neutrinos correlated with GRBs would therefore be a “smoking-gun” signal for UHECR acceleration in GRBs but up to now, no prompt neutrino signal has been detected either by IceCube or by Antares [7, 8, 9, 10].

We describe in the following a new search method for detecting these neutrinos using the IceCube Neutrino Observatory. IceCube is a cubic-kilometer neutrino detector installed in the ice at the geographic South Pole [11] between depths of 1450 m and 2450 m. Detector construction started in 2005 and finished in 2010. Neutrino reconstruction relies on the optical detection of Cherenkov radiation emitted by secondary particles produced in neutrino interactions in the surrounding ice or the nearby bedrock. We aim to analyse four years of data of the fully completed detector (from May 13th, 2011 to May 18th, 2015) for all the GRBs located in the Northern hemisphere during this period.

2. Gamma ray bursts

GRBs are short, unexpected and principally non-thermal bursts of γ -rays. In terms of duration, a “typical” GRB lasts for $\mathcal{O}(10\text{s})$ but it can vary from the millisecond scale to thousands of seconds, as can be seen in Fig. 1. Early hints [12] provided indications that GRBs can be separated into 2 categories according to their duration, which was confirmed with the observations performed with the BATSE satellite [13]. The 2 distinctive types are: short GRBs (SGRBs) with $T_{90} \leq 2\text{s}$ and long GRBs (LGRBs) with $T_{90} > 2\text{s}$, where T_{90} is defined as the time needed to accumulate from 5% to 95% of the fluence in the 50 – 300 keV band. This separation is clearly visible in Fig. 1. This segregation of GRBs cannot be attributed to an instrumental artefact but it represents a real physical property [13]. Both subpopulations are indeed isotropically distributed on the sky as expected from two independent uniform distributions of extra-galactic objects. The observed GRB population consists of about 30% of SGRBs and 70% of LGRBs.

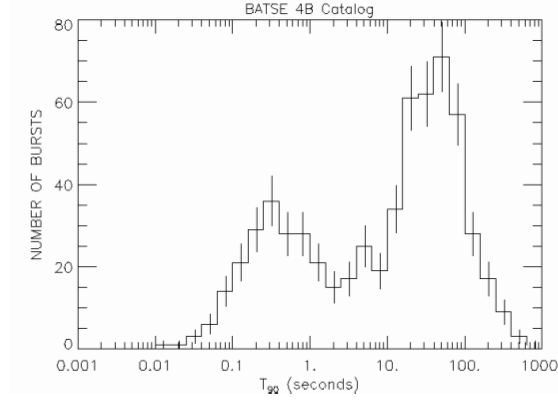


Figure 1: Distribution of T_{90} for 1234 GRBs in the BATSE 4B Catalog. From [14].

Evidence points to GRBs being the visible part of catastrophic energy release in stellar massive objects. However, a complete understanding of the different stages involved in the GRB phenomenon is still missing. In this context, the observation of two duration classes may indicate different progenitors. It is believed that the LGRBs are almost surely associated to the “death” of a massive star, *i.e.* the collapse of its core, leading to the so-called collapsar model [15]. This is supported by associations of GRBs with supernova events [16]. The picture is less settled yet for the SGRBs, but there are some observational indications [17, 18] that SGRBs could be associated with compact binary mergers [19] of two neutron stars or of a neutron star with a black hole. However, the generic evolution of the explosion after the initial energy injection is most probably independent of the progenitor. The “inner engine” would only have some influence on the variability of the light curves of the GRB [20].

As explained in the introduction, neutrinos are also expected to be created by GRBs. These neutrinos may be produced during three consecutive phases with respect to the gamma flash: precursor (before the actual GRB), prompt (during the emission of gamma-rays) and afterglow. This variety of signals makes the timing signature of the neutrino very complex and therefore makes it difficult to link with a gamma observation. We also expect a broad range of possible emission spectra for each of these specific phases [14]. For SGRBs, it has been shown that the produced neutrino spectrum is expected to be harder than E^{-2} because the very high accelerating gradients needed in these objects, will accelerate the muons before their decay [21]. We therefore intend to perform an analysis based on very generic models. In this context, the physical information of a separation of the GRBs in two subclasses in terms of their duration offers the opportunity to enhance the significance for a time spectral analysis.

3. Data samples and event selection

For developing the event selection of our analysis according to the IceCube blindness policy, we use an off-source burn sample as background estimation composed of 48 data samples of 2 consecutive hours during 4 years (from May 13th, 2011 to May 18th, 2015) of real data without a known GRB. Each data sample corresponds to each month of the considered period, to account for the seasonal variations in the cosmic ray intensity [22]. The signal is modelled by a Monte Carlo

simulation of a generic expected signal spectrum of E^{-2} , corresponding to the well-known Fermi acceleration mechanism. The analysis has been optimised for “well-reconstructed” signal¹.

The first phase of the event selection consists of a newly developed criterion which selects the muon tracks that are most likely up-going in the detector, *i.e.* particles coming from the Northern hemisphere. This method is based on the combination of several track reconstruction methods in order to select more efficiently the up-going tracks. After this first selection, a Boosted Decision Tree (BDT) is trained on the data and allows us to reduce the background data to the mHz scale (atmospheric neutrino flux scale) while keeping up to $\sim 90\%$ of the well-reconstructed simulated signal events. This leads to an effective area shown in Fig. 2, where this observable is defined as the ratio of the observed event rate and the incoming neutrino flux. As such the effective area, obtained from simulations, provides a means to relate our observations with the actual neutrino flux. We see that we improve the event selection compared with the latest IceCube analysis [10] with a gain especially in the low energy regime. This will lead to an increase of events that pass the developed event selection. Furthermore, the 1σ angular resolution of the passing signal events is $\Delta\Psi = 1.35^\circ$, which is comparable with the previous analysis [10]. Note that the effective area and angular resolution values are given after a cut on the BDT score leading to a signal efficiency of 85% and a signal purity of 86%.

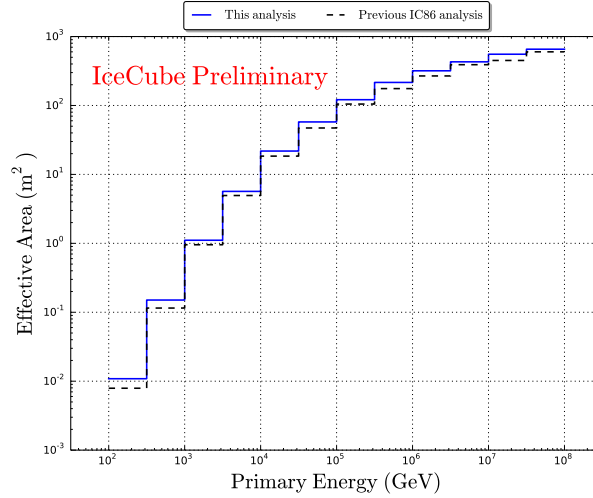


Figure 2: Effective area of the expected neutrino signal for an E^{-2} spectrum as a function of the neutrino energy. The blue line represents this analysis and the black dotted line the latest IceCube result performed with the full detector [10].

4. Statistical analysis

4.1 Short GRBs

In the case of short GRBs, a simple cut and count experiment has been performed. This

¹In IceCube, each physical event is reconstructed by different algorithms, leading to several possible reconstructed tracks. Here, we define well-reconstructed signal as having one of these reconstructed tracks in a 5° angular window around the simulated direction.

method aims to detect possible prompt neutrinos from GRBs. This analysis is based on a stacking procedure for all the SGRBs in the considered period, which amounts to 82 for the 4 considered years.

The analysis is composed of two different cuts that are performed on the data:

- Time cut: a time window of 4 s beginning 1 s before the starting time of the GRB ;
- Spatial cut: an angular window given by the square root of the quadratic sum of the GRB angular uncertainty and the reconstruction precision.

The passing events are then stacked for all GRBs and the test statistic applied is the Poisson distribution.

In order to determine the mean value of the background Poisson distribution and to extract the method sensitivity and the discovery potential limits for each of the BDT score cut thresholds, a null hypothesis experiment is performed. It consists of pseudo-experiments that have been performed by randomising the GRB azimuth angles and the event starting times. Finally, signal is injected to determine the BDT cut by optimising for discovery the fluence normalisation F_0 , for a generic E^{-2} spectrum and for a Waxman-Bahcall spectrum with a first energy break at $\varepsilon = 10^6$ GeV [10]. This procedure is applied for different BDT score thresholds, ranging from 0.05 to 0.25 in steps of 0.01. The 4 years results are presented in Fig. 3. The optimisation of the BDT cut for obtaining the best sensitivity instead of optimisation for discovery gives very similar results.

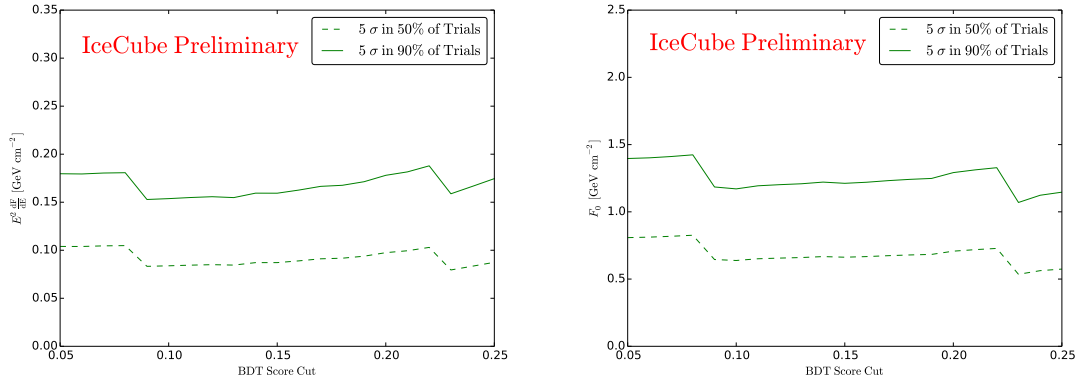


Figure 3: Fluence normalisation factor in function of the BDT score threshold for generic E^{-2} spectrum (left) and in the case of a Waxman-Bahcall spectrum [10] (right).

The results shown in Fig. 3 are competitive compared to previous IceCube analyses [10] and they are the first discovery potential limits reported for a short GRB search. We see that whereas the chosen spectrum has an impact on the fluence normalisation factor it is independent for the optimisation of the BDT cut. We propose a cut at $\text{BDT}_{\text{score}} \sim 0.10$. This is the loosest cut which is still in the discovery potential signal optimum plateau for both spectrums.

An extension of the method, analysing the time difference between observed events, will be performed in the future to be also sensitive to precursor and afterglow neutrinos.

4.2 Long GRBs

In order to determine the best statistical method for the detection of neutrinos from LGRBs, several methods were compared using a toy model simulation of the arrival times and locations of background and signal events. Previous searches using the complete IceCube detector have been tailored for prompt neutrinos [10]. This analysis aims at being sensitive to the three neutrino emission phases (precursor, prompt and afterglow) mentioned before. For this purpose, a time window around the GRB trigger time as well as an angular window around the GRB position are defined. One is limited in the choice of such windows since a too large window would increase the background and reduce the sensitivity of the method. Hence, an analysis cannot be sensitive to all possible precursor and afterglow times.

In this analysis, we have chosen to consider a time window of one hour around the trigger time of GRBs and an angular window of 15° around each GRB position. These choices are the results of an optimisation based on the different statistical methods used. Our toy model simulation generates signal and background events corresponding to the 491 LGRBs of the four years data sample taking into account position and reconstruction uncertainties, duration and redshift effects. After the numerical event generation, the time and angular windows around the 491 simulated GRBs are stacked in a similar way as outlined in [24].

Two observables were simulated, the time between an observed muon and the associated GRB trigger time and the angular distance between the associated GRB position and the reconstructed direction of the events. The background event generation is uniform in time and isotropically distributed. For every signal event, the characteristics (T_{90} , angular uncertainty and redshift) of a GRB are chosen randomly from the list of GRBs.

The prompt signal event time is generated following a flat distribution during the γ emission of the selected GRB (T_{90}) to which Gaussian tails are added on each side. In the precursor case, the signal event time is generated exactly 2 minutes before the GRB trigger time at the source. The actual event time of these precursor events varies as function of the GRB redshift. The angular distribution of signal events follows a Gaussian distribution with a standard deviation in which the median angular resolution of this analysis and the uncertainty on the selected GRB position are taken into account.

The method previously used in IceCube²[10] and hereafter named “Likelihood” defines the test-statistic T as

$$T = \sup_{n_s} \left[-n_s + \sum_{i=1}^{N_{\text{event}}} \log \left(\frac{n_s S_i}{\langle n_b \rangle B_i} + 1 \right) \right], \quad (4.1)$$

where $S = S_{\text{time}} \times S_{\text{angle}}$ indicates the signal Probability Density Function (PDF) and $B = B_{\text{time}} \times B_{\text{angle}}$ the background one. S_{time} and S_{angle} are the same distributions as the ones used to generate the signal events. The background distribution B_{time} is uniform in time and the background angular distribution B_{angle} follows the solid angle effect. The parameters n_s and $\langle n_b \rangle$ are the number of source neutrinos and the expected number of background events, respectively.

²In previous GRB analyses an energy spectrum was also considered in the Likelihood method to further distinguish background and signal events. We made the choice of not using an energy distribution in order to avoid biases towards higher energy events.

The Likelihood method is compared to another method called hereafter “PLT”, which is defined in [23]. This method considers the signal as a perturbation of the background. If the strength of this perturbation is η and its location in time or in angle is θ , we can define

$$p(x|\eta, \theta) = (1 - \eta)B(x) + \eta S(x|\theta) \quad (4.2)$$

and

$$S(\theta) = \frac{\partial \log \left[\prod_{i=1}^{N_{\text{events}}} p(t_i|\eta, \theta) \right]}{\partial \eta} \Big|_{\eta=0}, \quad (4.3)$$

where, as above, B is the background PDF and S is the signal one.

The test statistic is then defined as $T = \sup_{\theta} S(\theta)$. Such a definition can be interpreted as a “scanning” of the parameter θ in order to find the location where the perturbation is the strongest. This method should be sensitive to the three GRB phases while the Likelihood method can only be used for a prompt neutrino search.

The obtained results, shown in Fig. 4 indicate that the PLT method is only slightly more sensitive to a precursor signal than the Likelihood method. Furthermore, the PLT method can detect more efficiently weak signals but becomes less sensitive than the Likelihood method when the signal strength increases.

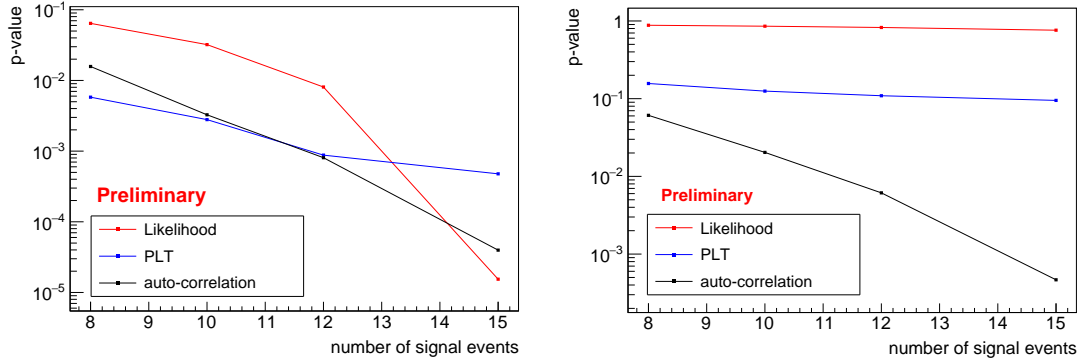


Figure 4: The p-value obtained from the three statistical methods described in the text, Likelihood in red, PLT in blue and the auto-correlation in black. The p-value is drawn in function of the number of signal events injected in the simulation. The left figure shows the prompt signal case and the right one considers a precursor signal. The background rate in this simulation is 3 mHz.

Another possibility under study consists of using a hybrid method using one of the likelihood methods described above for the angular part (for PLT, θ would then be the angle between the GRBs and the events) and the auto-correlation method for the time part. In the auto-correlation method we generate a distribution with the time differences between all possible event pairs. The distribution is then binned and the number of pairs per bin is compared to a background only simulation in order to extract the probability of having a certain number of pairs in a specific bin. The lowest probability of all the bins is reported as the test statistic. Since the sensitivity of the method depends on the binning choice, an optimisation has been performed in order to select the most appropriate binning. The auto-correlation is presented with the PLT and the Likelihood method on Fig. 4.

The hybrid method would have the strength of a likelihood method for the angle distribution as well as a sensitivity for all GRB phases. The sensitivity of the auto-correlation method to both prompt and precursor events, as can be seen on Fig. 4 is due to the unnecessary of defining a signal PDF.

5. Conclusion

We have developed a new search for neutrinos from GRBs based on two dedicated methods for LGRBs and SGRBs. For the first time, the SGRBs has been studied separately and the results are promising. The discovery potential limits are competitive compared to previous IceCube analysis. An effort will be devoted in the near future to develop a statistical analysis sensitive to all the possible phases of neutrino emissions (precursor, prompt and afterglow).

In the case of the LGRBs search, in which signal events are expected in a broader time window, dedicated statistical tools are being investigated. As in the case of SGRBs, we aim to define a method sensitive to the three possible phases of neutrino emissions. We expect that the optimisation of the statistical method both for long and short GRBs combined with a more efficient event selection can result in a neutrino detection in relation with a GRB or in stringent upper-limits on the neutrino flux.

References

- [1] M. Vietri, *Astrophys. J.* **453** (1995) 883.
- [2] E. Waxman, *Phys. Rev. Lett.* **75** (1995) 386.
- [3] A. Shemi and T. Piran, *Astrophys. J.* **453** (1990) L55.
- [4] T. Piran, *Rev. Mod. Phys.* **76** (2004) 1143
- [5] P. Mészáros, *Rept. Prog. Phys.* **69** (2006) 2259.
- [6] E. Waxman and J. Bahcall, *Phys. Rev. Lett.* **78** (1997) 2292.
- [7] **IceCube** Collaboration, R. Abbasi *et al.*, *Phys. Rev. Lett.* **106** (2011) 141101.
- [8] **IceCube** Collaboration, R. Abbasi *et al.*, *Nature* **484** (2012) 351.
- [9] **Antares** Collaboration, S. Adrián-Martínez *et al.*, *A&A* **559** (2013) A9.
- [10] **IceCube** Collaboration, M. G. Aartsen *et al.*, *Astrophys. J.* **805** (2015) L5.
- [11] **IceCube** Collaboration, A. Achterberg *et al.*, *Astropart. Phys.* **26** (2006) 155.
- [12] K. Hurley, *AIP Conf. Proc.* **265** (1991) 3.
- [13] C. Kouveliotou *et al.*, *Astrophys. J.* **413** (1993) L101.
- [14] J. K. Becker, *Phys. Rept.* **458** (2008) 173.
- [15] S. E. Woosley, *Astrophys. J.* **405** (1993) 273.
- [16] J. Hjorth *et al.*, *Nature* **423** (2003) 847-850.
- [17] D. B. Fox *et al.*, *Nature* **437** (2005) 845.
- [18] E. Berger *et al.*, *Nature* **438** (2005) 988.
- [19] B. Paczynski, *Astrophys. J.* **308** (1986) L43.
- [20] S. Kobayashi *et al.*, *Astrophys. J.* **490** (1997) 92.
- [21] S. R. Klein, *Astrophys. J.* **779** (2013) 106.
- [22] **IceCube** Collaboration, S. Tilav *et al.*, *Atmospheric Variations as observed by IceCube*, in *Proc. of the 31st ICRC* (2009) Lodz, Poland.
- [23] R. Pilla, C. Loader, and C. Taylor, *Phys. Rev. Lett.* **95**.
- [24] N. van Eijndhoven, *Astroparticle Physics* **28** (2008) 540.

Neutrino-triggered target-of-opportunity programs in IceCube

The IceCube Collaboration[†],

[†] http://icecube.wisc.edu/collaboration/authors/icrc15_icecube

E-mail: Dariusz.Gora@desy.de

IceCube is capable of monitoring the whole sky continuously, while optical and high energy photon telescopes have limited fields of view and are not likely to observe a potential neutrino-flaring source at the time such neutrinos are recorded. The use of neutrino-triggered alerts thus aims at increasing the availability of simultaneous multi-messenger data, which can increase the discovery potential as well as constrain the phenomenological interpretation of the high energy emission of selected source classes. The requirements of a fast and stable online analysis of potential neutrino signals and its operation will be discussed. The status and the recent improvements of a neutrino-triggered program in IceCube are described. The currently running systems generate real-time alerts based on multiplets of neutrinos occurring close in time and space, and these alerts are received for follow-up observations by various instruments, ranging from optical (PTF) and X-ray (Swift) to gamma-ray (H.E.S.S., MAGIC and VERITAS). The possibility in the near future to additionally send alerts based on single high energy neutrino events of likely astrophysical origin will also be discussed.

Corresponding authors: Dariusz Góra^{1*}, Elisa Bernardini^{1,2}, Marek Kowalski^{1,2}, Markus Voge³, Alexander Stasik², Thomas Kintscher¹

¹ *Institut für Physik, Humboldt Universität, Newtonstr. 15, D-12489 Berlin, Germany*

² *Deutsches Elektronen-Synchrotron (DESY), Platanenallee 6, D-15735 Zeuthen, Germany*

³ *Physikalisches Institut, Universität Bonn, Nussallee 12, D-53115 Bonn, Germany*

*The 34th International Cosmic Ray Conference,
30 July- 6 August, 2015
The Hague, The Netherlands*

*Speaker.

1. Introduction

Neutrinos have long been anticipated to help answer some fundamental questions in astrophysics like the mystery of the source of the cosmic rays (for a general discussion see [1]). For neutrinos in the TeV range, prime source candidates are Galactic supernova remnants [2]. Neutrinos in the PeV range and above are suspected to be produced by Active Galactic Nuclei (AGN) and Gamma Ray Bursts (GRB) with many AGN models predicting a significant neutrino flux [3, 4, 5]. Recently, the IceCube Collaboration has reported the very first observation of a cosmic diffuse neutrino flux which lies in the 100 TeV to PeV range [6]. Individual sources, however, have not been identified. While many astrophysical sources of origin have been suggested, there is yet not enough information to narrow down the possibilities to any particular source.

The detection of cosmic neutrinos by high-energy neutrino telescopes is very challenging due to the small neutrino interaction cross-section and because of a large background of atmospheric neutrinos. Thus, simultaneous measurements using neutrino and electromagnetic observations (the so-called “multi-messenger” approach) can increase the chance to discover the first neutrino signals from astrophysical source by reducing the trial factor penalty arising from the observation of multiple sky regions over different time periods.

For slower transient sources like AGNs (time scale of weeks) which manifest large time variations in the emitted electromagnetic radiation, the signal-to-noise ratio can be increased by searching for periods of enhanced neutrino emission (a time-dependent search). Of special interest is the relation of these periods of enhanced neutrino emission with periods of strong high-energy γ -ray emission. However, as Imaging Air Cherenkov Telescopes (IACTs) such as MAGIC [7] or VERITAS [8] have a small field-of-view and are not continuously operated such correlation studies are not always possible after the flare. Therefore it is desirable to ensure the availability of simultaneous neutrino and high-energy γ -ray data for periods of interests. This is achieved by an online neutrino flare search that alerts a partner IACT experiment when an elevated rate of neutrino events from the direction of a source candidate is detected. Such a Neutrino Triggered Target of Opportunity program (NToO) using a list of pre-defined sources was developed already in 2006 using the AMANDA neutrino telescope to initiate quasi-simultaneous gamma-ray follow-up (GFU) observations by MAGIC [9]. The refined and enhanced implementation of GFU, using the data from IceCube neutrino detector to send alerts to γ -ray telescopes MAGIC and VERITAS, was started on March, 2012 [10].

Similarly, one can conduct a search for neutrinos from short transient sources (time scale of 100 seconds), such as GRBs (see e.g. [11]) and core-collapse Supernovae (SNe) (see e.g. [12]). These sources are most accessible in X-ray and optical wavelengths, where one can observe the GRB afterglow or the rising SN light curve, respectively. As for IACTs, the field of view and observation time of X-ray and optical telescopes is limited. Since identification of a GRB or SN is only possible within a certain time range (few hours after a GRB and few weeks after a SN explosion), it is important to obtain electro-magnetic data within these time frames. Therefore, another NToO program targeting optical (OFU) and X-ray (XFU) follow-up of short neutrino transients has been developed as well since 2008 [10, 13]. Upon multiplets (at least 2) of neutrinos within 100 seconds and 3.5° angular separation (searching anywhere in the sky), alerts are sent to ROTSE [14], PTF [15] for optical and Swift [16] for X-ray follow-up, depending on the multiplet’s significance.

2. Selection of Target Sources

As already mentioned, the online search for short transient neutrino sources is mostly motivated by models of neutrinos from long durations GRBs [11] and from choked jet supernovae (SNe) [12] that are SNe hosting a mildly relativistic jet. The two source classes are related: Both are thought to host a jet, which is highly relativistic in case of long GRBs, but only mildly relativistic in case of choked jet SNe. However, the choked jet is less energetic and thus cannot penetrate the stellar envelope, making it invisible in γ -rays. The produced neutrinos at TeV energies can escape nevertheless and might trigger a discovery of a SN in the follow-up channels. Both sources are expected to emit a short, about 10 s long burst of neutrinos either 10 to 100 s before or at the time of the γ -ray burst, setting the natural timescale of the neutrino search. After recording the neutrino burst, follow-up observations can be used to identify the counterpart of the transient neutrino source. The γ -ray burst itself is generally too short for a follow-up to IceCube data, since 95% of GRBs have a duration of less than 150 s. However, there are good detection prospects using the GRB afterglow, in optical or in X-ray data. A very fast response within minutes to hours is required for this. A choked jet SN is found by detecting a shock breakout or a SN light curve in the follow-up images, slowly rising and then decaying within weeks after the neutrino burst. In addition to the transient neutrino emission within 100 s, as discussed above, SNe can be promising sources of high-energy neutrinos, especially the class of Type IIn SNe [17]. These are core-collapse SNe embedded in a dense circumstellar medium (CSM) that was ejected in a pre-explosion phase. Following the explosion, the SN ejecta plow through the dense CSM and collision less shocks can form and accelerate particles, which may create high-energy neutrinos. This is comparable to a SN remnant, but on a much shorter time scale of 1 to 10 months.

Coordinated observation of gamma-rays and neutrinos might be possible for sources where charged and neutral mesons are produced simultaneously, from hadronic p-p or p- γ interactions. This concerns variable objects such as Blazars or Flat-Spectrum Radio Quasars (FSRQs), as well as Galactic systems like microquasars and magnetars, whose emission is interpretable with hadronic models. The chance of detection of individual AGN flares, on a time scale of days or weeks, is estimated on different predictions for the mechanism yielding the observed electromagnetic emission at high energies [3, 4]. A common feature of several models is that the class of high energy peaked BL Lacs (HBLs) is expected to be weakest in neutrinos, as compared to low energy peaked BL Lacs (LBLs) and FSRQs, if interactions of protons with ambient or self-produced radiation significantly contribute to the observed high energy gamma-ray emission. With high target matter density, the neutrino yield can be highest when the very high energy γ -ray emission is strongly attenuated by internal absorption, with cut-off values, however, being uncertain. In case of pp-dominated scenarios, conclusions are different [4], favoring LBLs to FSRQs. In all cases, the availability of simultaneous information on high energy γ -ray emission and neutrinos is crucial.

The most interesting objects as a target for GFU observations triggered by IceCube events are promising sources of TeV neutrinos, which are either known to exhibit a bright GeV flux in γ -rays and show extrapolated fluxes detectable by IACTs, or are already detected by IACTs and are variable. Thus, for GFU the selected list of AGNs from the second Fermi point-source catalog [20] combined with the lists provided by the partner experiments (currently MAGIC and VERITAS) covering the Northern hemisphere ($\delta > 0^\circ$) are used, see [10] for more details.

3. The IceCube follow-up alert issuing system

IceCube is a cubic-kilometer neutrino detector installed in the ice at the geographic South Pole [21] between depths of 1450 m and 2450 m. Detector construction started in 2005 and finished in December 2010. Neutrino reconstruction relies on the optical detection of Cherenkov radiation emitted by secondary particles produced in neutrino interactions in the surrounding ice or the nearby bedrock. For NToO programs presented here, only muon neutrino events are considered, because of the long range of the secondary muons which allows for reconstructing these events with good pointing accuracy. The pointing information relies on the secondary muon direction, which at energies above 1 TeV differs from the original neutrino direction by less than the angular resolution of the detector. The current online data processing is running in real-time within the limited computing resources at the South Pole, capable of reconstructing and filtering the neutrinos and sending alerts to follow-up instruments with a latency of only a few minutes. The optical (OFU) and X-ray (XFU) real-time follow-up programs currently encompass three follow-up instruments: the Robotic Optical Transient Search Experiment (ROTSE) [14]¹, the Palomar Transient Factory (PTF) [15] and the Swift satellite [16]. These triggered observations were supplemented with a retrospective search through the Pan-STARRS1 3π survey data [18]. Similarly, the GFU is sending alerts to the MAGIC and VERITAS.

The basis for the neutrino event selection is an on-line filter that searches for high-quality muon tracks. The fullsky rate of this filter is about 40 Hz for IceCube in its 2012/2013 configuration with 86 deployed strings. This rate is strongly dominated by atmospheric muons. In order to efficiently select neutrinos events from this sample several elaborate reconstruction algorithm have to be applied. However, as the computing resources at the South Pole are limited, this is only possible at a lower event rate. The so-called Online Level 2 Filter (Online-L2 Filter) selects events that were reconstructed as upgoing with a likelihood reconstruction that takes into account the time of arrival of the first photon at each Digital Optical Module (DOM) and the total charge recorded in that module. By requiring a good reconstruction quality the background of misreconstructed atmospheric muons is reduced. The parameters used to assess the track quality are the likelihood of the track reconstruction, the number of unscattered photons with a small time residual w.r.t. the Cherenkov cone and the distribution of these photons along the track. The reduced event rate of approximately 5 Hz can then be reconstructed with more time intensive reconstructions, like angular resolution estimators and likelihood fits applied to different subsets of the recorded photons. Based on these reconstructions the final event sample is selected by employing different quality cuts for OFU/XFU and GFU. The event selection results in an event rate of about 2 mHz for GFU and 3mHz for OFU and a median angular resolution of 0.6° for 100 TeV and higher energies.

For OFU/XFU, in order to suppress background from atmospheric neutrinos, a multiplet of at least two neutrinos within 100 seconds and angular separation of 3.5° or less is required to trigger an alert. In addition, since 2011 mid-September, a test statistic is used, providing a single parameter for selection of the most significant alerts. It was derived as the analytic maximization of a likelihood ratio following [19], for the special case of a neutrino doublet with rich signal content, see [10] for more details.

For GFU the timescale of a neutrino flare is not fixed a-priori, and the time-clustering ap-

¹At the moment, there is no followup to ROTSE anymore as they went out of operation.

proach that was developed for an unbiased neutrino flare search [22] looks for any time frame with a significant deviation of the number of detected neutrinos from the expected background. The simplest implementation uses a binned approach where neutrino candidates within a fixed radius around a source are regarded as possible signal event. If the significance for an evaluated event cluster exceeds a certain threshold, an alert message containing the source name, event positions, event times and the significance of the cluster is generated and the sent to partner experiments, see also [10] for more detailed description of GFU.

4. Selected results of NToO programs

The IceCube NToO programs like OFU/XFU/GFU have been running stably for a few years and are taking high-quality data from both IceCube and the follow-up instruments. The result will be subject of forthcoming publications [24]. Thus here, only a short status report will be given, highlighting the most important results.

For OFU/XFU, the total number of observed doublet alerts is 258, since inauguration of the program in December 2008 until May 2014. This stands against a background expectation of 236.7 ± 15.4 doublets. No triplets have been observed, while the background expectation is 0.09 ± 0.3 triplets. However, in March 2012, the most significant neutrino alert during the first three years of operation was issued by IceCube. In the follow-up observations performed by the PTF, a Type II_n supernova (SN) PTF12csy was found 0.2° away from the neutrino alert direction, with an error radius of 0.54° . It has a redshift of $z = 0.0684$, corresponding to a luminosity distance of about 300 Mpc and the Pan-STARRS1 survey shows that its explosion time was at least 158 days (in host galaxy rest frame) before the neutrino alert, so that a causal connection is unlikely. The a posteriori significance of the chance detection of both the neutrinos and the SN at any epoch is 2.2σ within IceCube's 2011/12 data acquisition season. Also, a complementary neutrino analysis reveals no long-term signal over the course of one year. Therefore, the SN detection is considered coincidental and the neutrinos uncorrelated to the SN. However, the SN is unusual and interesting by itself: It is luminous and energetic, bearing strong resemblance to the SN II_n 2010jl, and shows signs of interaction of the SN ejecta with a dense circumstellar medium. High-energy neutrino emission is expected in models of diffusive shock acceleration, but at a low, non-detectable level by IceCube experiment for this specific SN.

For GFU, since the inauguration of the GFU program in 2012, 13 physics alerts have been sent so far (4 in 2012, 2 in 2013, 6 in 2014, 2 in 2015). Follow-up observations have been performed by MAGIC in three cases and by VERITAS in four cases. The most interesting alert generated on 9 November 2012 originated from the source 1150+497 (located at $\theta = 139.5^\circ$). Six events observed during 4.169 days comprise the alert. The Poisson probability (pre-trial) for this observation is $-\log_{10} p = 4.64$, the highest alert significance of the alerts sent during the 2012/2013 data acquisition season. The alert was forwarded to the VERITAS telescope and resulted in a follow-up observation. The VERITAS team received the alert from IceCube, but due to the poor weather and bright moonlight conditions did not allow VERITAS observations until 12 November 2012, at which point the source was visible at low elevations at the very end of the night. A further observation was made on the following night with the total exposure time of about 15 min. No statistically significant evidence for gamma-ray emission was seen from the position of source, thus the integral upper flux limit was calculated by VERITAS.

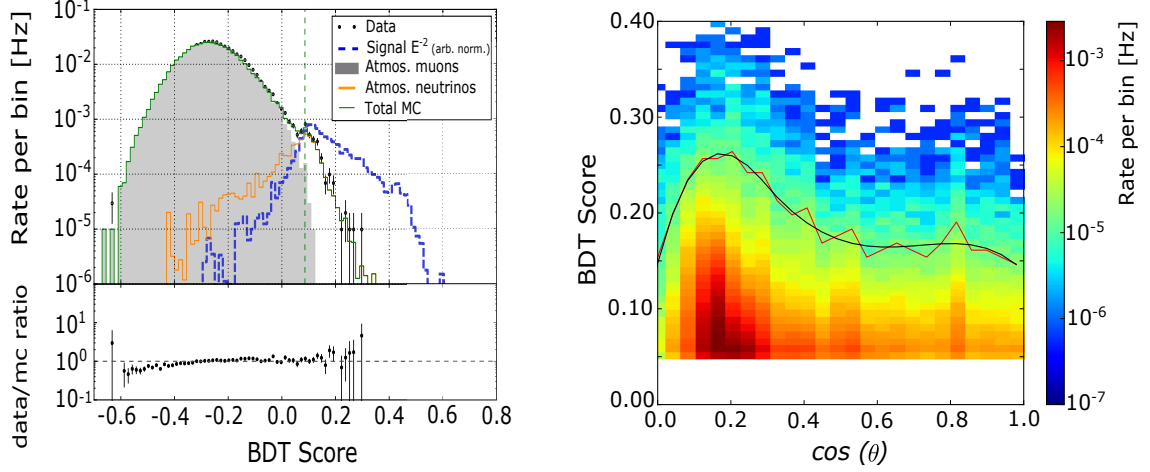


Figure 1: (A) Distribution of BDT score for the ensemble of trees trained with an E^{-2} spectrum. Vertical dashed lines corresponds to optimized BDT cut (Northern hemisphere). (B) The BDT score as a function of $\cos(\text{zenith angle})$. The red lines keeps approximately an equal rate per zenith bin ($\simeq 10^{-4}$ Hz). A piecewise polynomial function is then fit to the red curve (black curve).

5. Recent and upcoming improvements

The currently deployed neutrino event selection in the GFU employs simple cuts on a number of variables that discriminate between signal neutrinos and atmospheric muon background. The cuts on these parameters have been optimized to achieve an optimal sensitivity. However, such cuts most likely do not lead to the most optimal shape in terms of signal and background separation. In order to increase the separation between signal and background event distributions the Boosted Decision Trees (BDTs) [23], multi-variate learning machines, were used. In fact, for (OFU/XFU) the multi-variant selection scheme was already implemented since 2012, but it was used to cover only the Northern Hemisphere. The aim is replacing the present GFU selection by developing a new event selection, which can be used also by OFU/XFU program, will be comparable to offline point source samples and will cover the entire sky i.e. providing 4π coverage. Here, a short description of a new BDT selection is presented, which has been implemented for 2015/2016 IceCube data acquisition season.

For a new BDT selection scheme, the multivariate cuts were based on 14 observables obtained by choosing parameters with low correlation in background but high discriminating power between signal and background. Observables specifying the geometry, the time evolution of the hit pattern as well as the quality and consistency of the various track reconstructions and the number of strings with signals are used. The BDT training was done with simulated signal events for a soft neutrino spectrum of $E^{-2.7}$ and for an E^{-2} spectrum. As an example, Figure 1 depicts results of the BDT training for an E^{-2} spectrum. In addition, to achieve a good result for all spectra, a new event weighting scheme was introduced, by giving each signal event a combined weight of the spectra weights (CSW): $w_i = (\frac{w_i^{E^{-2.7}}}{\sum_j w_j^{E^{-2.7}}} + \frac{w_i^{E^{-2}}}{\sum_j w_j^{E^{-2}}} + \frac{w_i^{E^{-1}}}{\sum_j w_j^{E^{-1}}}) / \sum_j w_i$. A set of off-time real data, was used for training as background. Additionally, for the simulated signal, the reconstructed track was required to be within of 5° of the simulated direction in order to train BDT with only well-reconstructed events. The final selections were optimized to provide the best discovery potential for an E^{-2} neutrino flux, which results in a BDT score value of 0.106. This final cut leads to a rate of 2 mHz for the final sample and as it shown in Table 1 to the better signal efficiency (w.r.t. to OnlineLevel-2

Cut Level	Data rate (mHz)	Atm. ν_μ rate (mHz)	E^{-1} Eff. (%)	E^{-2} Eff. (%)	$E^{-2.7}$ Eff. (%)
Simple Cuts	2.0	1.9	79	69	54
BDT $E^{-2.0}$	1.9	1.7	86	81	72
BDT $E^{-2.7}$	2.7	2.5	84	78	65
BDT CSW	3.1	2.8	83	80	72

Table 1: Data, atmospheric muon, and neutrino expected background rates for different cut progression. The signal efficiency for an E^{-2} neutrino spectrum with respect to the OnlineL2 Filter is also shown.

Filter efficiency) than the straight GFU cuts. The BDT-based event selection leads to the improvement in the signal efficiency of about +11(+18)% for an E^{-2} ($E^{-2.7}$) spectrum w.r.t. the simple cuts.

The BDT selection was also used for the Southern hemisphere (zenith angle $\theta < 90^\circ$). However instead of a single BDT score cut value, a zenith-dependent cut was applied in order to select a constant number of events per solid angle, as it is shown in Figure 1 (B). This zenith-dependent cut was also optimized w.r.t. sensitivity and discovery potential for an E^{-2} neutrino spectrum. The optimized cut described by a polynomial fit (Figure 1 (B)) leads to the total data rate of 2.1 mHz and average signal efficiency of about 40 % (w.r.t. OnlineL2 Filter).

It was the first step in establishing the GFU, demonstrating its technical feasibility and proving that a time-dependent point source search can be run stably and reliably over long periods of time at the South Pole. Therefore a simple search technique like the binned method was implemented first. However, current offline IceCube searches for neutrino point-sources usually employ unbinned maximum likelihood methods [19] to increase the discovery potential. Thus, also for GFU such an approach was implemented, in order to calculate the alert significance by taking into account an event-by-event angular reconstruction uncertainty estimation and an energy estimation of the event. The upgrade towards the BDT-based event selection and a subsequent likelihood analysis, in case of GFU increase the sensitivity in the Northern hemisphere of about 30-40% to a level comparable to the sensitivity obtained for the standard offline point-source analysis [25]. It also opens the possibility to observe flares on the Southern hemisphere and forward alerts to the H.E.S.S. telescope [26], with which an MoU has been established.

In previous years of operation of the OFU/XFU/GFU systems, neutrino candidate event selections, multiplet selection and alert generation all took place within the data acquisition system at South Pole. Although well-contained, it was found to be somewhat inflexible and difficult to expand. To address these shortcomings, the OFU/GFU/XFU systems are already transitioning to a new system. This system separates the neutrino candidate selection at the South Pole, and transmitting the information as a stream of single high energy events to North via rapid satellite communication channels. Followup processes in the North evaluate neutrino candidates, and generate alerts for external observatories, see [25] for more detailed description.

6. Conclusions

The IceCube NToO programs (OFU, XFU and GFU) have been running stably since a few years and are taking high-quality data from both IceCube and the follow-up instruments. As an example, the highest significance alert from the OFU program led to a coincidental discovery of a

Type II_n SN, demonstrating the capability of the follow-up system to reveal transient high energy neutrino sources. Several enhancements of NToO programs have recently been implemented (i.e. BDT selections and a maximum-likelihood based significance calculation) or are planned for the near future (i.e. the extension to the Southern hemisphere). The current online alert systems are limited to the Northern hemisphere due to the enormous atmospheric muon background. Finally, changes to the online followup framework, i.e. the stream of single high energy events, are under way. Hopefully, these improvements to NToO programs will help to identify sources of ultra-high energy neutrinos and in consequence the high energy astronomical phenomena which emit cosmic rays for a short (~ 100 s) or long (\sim weeks) period of time.

References

- [1] T.K Gaisser and T.Stanev, *Astropart. Phys.* **39-40** (2012) 120.
- [2] K. Koyama et al., *Nature* **378** (1995) 255.
- [3] A.M. Atoyan, C.Dermer, *New Astron. Rev.* **48** (2004) 381.
- [4] A. Neronov, M. Ribordy, *Phys. Rev. D* **80** (2009) 083008.
- [5] A. Mucke et al., *Astropart. Phys.* **18** (2003) 593.
- [6] M.G. Aartsen et al., *Science* **342** (2013) 1242856.
- [7] **MAGIC** Collaboration: <http://magic.mppmu.mpg.de/>.
- [8] **VERITAS** Collaboration: <http://veritas.sao.arizona.edu/>.
- [9] M. Ackermann et al., Proc. 29th ICRC (2005) [arXiv:astro-ph/0509330].
- [10] R. Abbasi et al., Proc. 32th ICRC (2013) [arXiv:1111.2741], M.G. Aartsen et al., Proc. 33th ICRC (2013) [arXiv:1309.6979].
- [11] E. Waxman, J. Bahcall, *Phys. Rev. Lett.*, **78** (1997) 2292.
- [12] S. Ando, J.F. Beacom, *Phys. Rev. Lett.*, **95** (2005) 061103.
- [13] R. Abbasi et al., *Astron. Astrophys.*, **A60** (2012) 539.
- [14] C.W. Akerlof et al., *Pub. of the Astro. Soc. of the Pacific* **115** (2003) 132.
- [15] N. Law et al., *Pub. of the Astro. Soc. of the Pacific* **121** (2009) 1395.
- [16] N. Gehrels et al., *The Astrophys. Journal* **611** (2004) 1005.
- [17] E.M. Schlegel *MNRAS* **244** (1990) 269; N. Smith et al., *The Astrophys. Journal* **143** (2012) 17.
- [18] N. Kaiser, *Proc. SPIE* 5489 (2004) 11; E.A. Magnier et al., *The Astrophys. Jour. Supp.* **205** (2013) 20.
- [19] J. Braun, M. Baker, J. Dumm et al., *Astropart. Phys.* **33** (2010) 175.
- [20] Fermi LAT Second Source Catalog: <http://heasarc.gsfc.nasa.gov/W3Browse/fermi/fermilpsc.html>.
- [21] A. Achterberg et al., *Astropart. Phys.* **26** (2006) 155.
- [22] K. Satalecka et al, for the **IceCube** Coll., *Proc. 30th ICRC* (2007) [arXiv:0711.0353].
- [23] S. S. Kerthi et al., *Neural Comp.* **13** (2001) 637.
- [24] M.G. Aartsen et al. *submitted to Astrophysical Journal* (2015) [arXiv:1506.03115].
- [25] **IceCube** Coll., paper 504 these proceedings.
- [26] <http://www.mpi-hd.mpg.de/hfm/HESS/>.

Low-energy (100 GeV - few TeV) neutrino point source searches in the southern sky with IceCube

The IceCube Collaboration[†]

[†] http://icecube.wisc.edu/collaboration/authors/icrc15_icecube

E-mail: rickard.strom@physics.uu.se

IceCube searches for neutrino point sources in the southern sky have traditionally been restricted to energies well above 100 TeV, where the background of down-going atmospheric muons becomes sufficiently low to be tolerated in searches. Recent developments of a data stream dedicated to the study of low-energy neutrinos from the Southern Hemisphere enable searches to be extended far below this threshold. This data stream utilizes powerful veto techniques to reduce the atmospheric muon background, allowing IceCube for the first time to perform a search for point-like sources of neutrinos in the southern sky at energies between 100 GeV and a few TeV. We will present the event selection along with the results obtained using one year of data from the full detector.

Corresponding authors: R. Ström^{1*},

¹ *Department of Physics and Astronomy, Uppsala University, Box 516, 751 20 Uppsala, Sweden*

*The 34th International Cosmic Ray Conference,
30 July- 6 August, 2015
The Hague, The Netherlands*

*Speaker.

1. Introduction

Neutrinos interact through gravity and the weak interaction only and can therefore, unlike other messenger particles like photons and protons, travel astronomical distances without experiencing significant absorption or deflection in magnetic fields. Further, they constitute a unique probe for distances larger than 50 Mpc and from extremely dense environments. This makes neutrinos ideal as cosmic messengers that can be used to explore the most powerful accelerators in the Universe, in particular the mechanisms for producing and accelerating cosmic rays to incredible energies.

By studying clustering of neutrino candidate events in the IceCube Neutrino Observatory (IceCube) we can discover sites of hadronic acceleration where neutrinos are produced in the decay of charged pions created when primary cosmic ray protons and nuclei interact with radiation and matter in the vicinity of the acceleration site.

The Southern Hemisphere is particularly interesting, containing both the Galactic Center and the main part of the Galactic plane. For IceCube this means we are studying down-going tracks in a much larger background of muons created as cosmic rays enter the Earth's atmosphere. The traditional workaround has been to study only the highest energy neutrinos well above 100 TeV, where the background of atmospheric muons is sufficiently low. In the LESE (Low Energy Starting Events) analysis presented in this contribution we have lowered the energy threshold significantly utilizing several veto techniques, i.e. by looking for starting events in the detector. In particular we study neutrinos from soft spectra with cut offs in TeV-scale as observed for Galactic γ -ray sources, see e.g. [1, 2, 3], and references therein.

2. Data and Simulation

IceCube instruments a cubic-kilometer of ice and is the world's largest neutrino telescope, located under the ice cap of the geographic South Pole, Antarctica [4]. It consists of 5160 optical modules deployed on 86 cables, called strings, and arranged in a three-dimensional grid between 1450 and 2450 m beneath the surface. The ultra pure ice at such depths is ideal for observations of Cherenkov light from charged leptons created when neutrinos interact with molecules in the ice or in the nearby bedrock.

Each optical module operates as an individual detector, a so-called DOM (Digital Optical Module), and consists of a photomultiplier tube, digitizer electronics and calibration LEDs, all housed in a pressure-resistant glass sphere. When two neighboring or next-to-neighboring DOMs on the same string both cross the 0.25 photoelectron discriminator threshold of the PMT within a $1 \mu\text{s}$ time window, the signals qualify to be in Hard Local Coincidence (HLC). The leading trigger condition is formed when at least eight DOMs with HLCs trigger within a $5 \mu\text{s}$ time window. In this analysis we also use events from a trigger dedicated to catching almost vertical events as well as one with a lower effective energy threshold active in a denser central subarray called DeepCore [5]. The total trigger rate considered is around 2.8 kHz. The data is reduced via a series of straight cuts dedicated to reconstruction and calorimetric quality and a cut on an event score calculated using a machine learning algorithm.

We present the analysis and results for data taken between May 2011 and May 2012, the first year of the completed 86-string IceCube detector. Runs were carefully selected to ensure that the

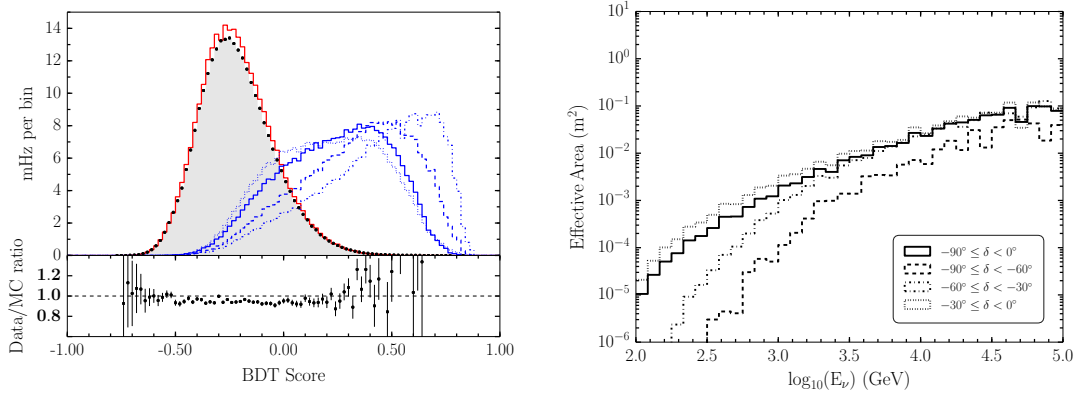


Figure 1: Left: BDT score distribution where experimental data is shown in black dots with error bars showing the statistical uncertainty (too small to be seen on this scale) and is further illustrated by the gray shaded area. Simulated atmospheric muons are presented in the solid red line. Signal hypotheses are shown in blue lines normalized to experimental data: E_ν^{-2} (dash-dotted), $E_\nu^{-2}e^{-E_\nu/10 \text{ TeV}}$ (dashed), $E_\nu^{-2}e^{-E_\nu/1 \text{ TeV}}$ (solid) and E_ν^{-3} (dotted). Simulated signals are defined as starting inside the instrumented detector volume. Right: Neutrino effective area as a function of neutrino energy.

majority of the DOMs used in vetoes were active, by both requiring a certain fraction of active DOMs overall and individually in the two different veto regions applied at the filter level, but also by studying the event rates at higher analysis levels. The final livetime considered is 329 days. The true right ascension directions of the data were kept blind until the last step of the analysis to keep the event selection and the final likelihood implementation as unbiased as possible.

3. Selecting Low-Energy Starting Events

The event selection is optimized for neutrinos in the energy region between 100 GeV to a few TeV. The outermost parts of the instrumented detector are used as a veto towards incoming muons. The triggered data is reduced by both real-time filtering at the South Pole, as well as subsequent offline CPU-intensive processing.

The development of a real-time full sky filter with a low energy threshold was crucial to reach lower energies, since many of the traditional IceCube real-time filters for the Southern Hemisphere were effectively using a charge cut, focusing on keeping events from 100 TeV and up. The filter consists of two steps: a hit pattern based part, that rejects events with recorded hits in any of the 5 top DOMs or with the first HLC hit on any of the outermost strings, followed by a rejection of events with a reconstructed interaction vertex outside of the fiducial volume¹. About 170 Hz pass the filter and is sent North for offline processing.

To ensure that we have enough information in the events for advanced angular and energy reconstructions we begin by considering overall quality cuts, such as a minimum required number of photoelectrons. We further reject events with a poor reconstruction quality. Several advanced vetoes are used to reduce the number of muons leaking in. In particular we are studying causality

¹ A polygon shaped region defined by connecting lines that go through points at 90% of the distance from the center string (string 36) to the outermost strings at the position of the 8 corners of the detector (as seen from the top) and the region below the 5 topmost DOMs.

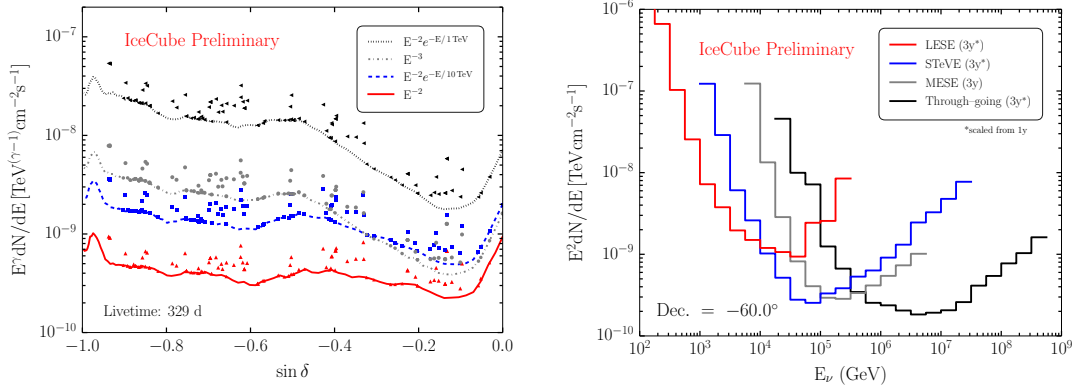


Figure 2: Left: Median sensitivities as a function of declination (line) and source upper limits (markers) at 90% C.L. Right: Differential median sensitivity corresponding to 3 years of operation (at -60° and 90° C.L.). Created by simulating point sources with an E^{-2} spectrum over quarter-decades in energy.

of hits in an extended veto region, consisting both of the outer regions of IceCube and the IceTop surface array [6].

As a major step in the event selection we apply a machine learning algorithm: a Boosted Decision Tree (BDT) is programmed to exploit the remaining separation between signal and background. In particular, it focuses on directional and calorimetric information. The BDT event score is shown in figure 1. We make a cut at 0.40 which was found to be optimal or close to optimal for a wide range of signal hypotheses.

The angular reconstruction uncertainty σ is estimated individually for each event as $\sigma^2 = (\sigma_1^2 + \sigma_2^2)/2$ where $\sigma_{1,2}$ are the major/minor axes of an ellipse that constitute the conic section of a paraboloid fitted to the likelihood space around the reconstruction minimum [7]. The ellipse is located at a level corresponding to 1σ indicating 68% containment. This quantity often underestimates the angular uncertainty, which is why we apply an energy dependent correction to the pull as seen in simulation, defined as the ratio of the true reconstruction error to the estimated reconstruction error, based on the median angular resolution. Events with a corrected value above 5° were rejected after optimization studies of the final sensitivity. The median angular resolution of the signal sample is about 2° .

The energy loss pattern for each event is estimated using an algorithm fitting hypothetical cascade-like energy depositions along the input track reconstruction [8]. An energy proxy for the neutrino energy is constructed by adding the contributions that are reconstructed inside the instrumented volume.

The final sample consists of 6191 events, a rate of about 0.2 mHz, and is still dominated by atmospheric muons leaking in through the veto layers, effectively mimicking starting events. The effective area for the full southern sky as well as in three declination bands is shown in figure 1.

4. Search for Clustering of Events

We look for point sources by searching for spacial clustering of events in the Southern Hemisphere. Hypotheses are tested using an unbinned maximum likelihood method [9] where the events

in the final sample contribute individually with their reconstructed position \mathbf{x}_i , reconstructed energy E_i and an estimation of the angular uncertainty σ_i . The likelihood \mathcal{L} is a function of two fit parameters: n_s (the number of signal events) and γ (spectral index of a source S located at position \mathbf{x}_S with an unbroken power law spectrum) and contains the probability for an event to be signal- or background-like. The final likelihood function is a sum over N events and is maximized with respect to n_s and γ where n_s is constrained to be non-negative:

$$\mathcal{L}(n_s, \gamma) = \prod_i \left(\frac{n_s}{N} \mathcal{S}_i(\mathbf{x}, \mathbf{x}_S; \sigma, E, \gamma) + \left(1 - \frac{n_s}{N}\right) \mathcal{B}_i(\delta; E) \right). \quad (4.1)$$

The signal PDF \mathcal{S} contains a spacial part parametrized with a two-dimensional gaussian profile with extension σ_i and since Icecube, due to its location, has a uniform acceptance in right ascension, the spacial part of the background PDF \mathcal{B} is represented with a spline fit to the full sample of experimental data depending on the declination δ only. The calorimetric parts of these PDFs consist of two-dimensional spline fits to the reconstructed energy E_i and declination δ_i .

The test statistic \mathcal{TS} used is the likelihood ratio Λ taken with respect to the null hypothesis ($n_s = 0$):

$$\mathcal{TS} = 2 \log \Lambda = \sum_i \log \left(1 + \frac{n_s}{N} \left(\frac{\mathcal{S}_i}{\mathcal{B}_i} \mathcal{W}_i - 1 \right) \right) \equiv \sum_i \log(1 + n_s \chi_i), \quad (4.2)$$

where χ_i is the individual event weight evaluated for a point source hypothesis at a particular location.

An all sky search is performed looking for an excess of neutrino candidate events in the Southern Hemisphere (declination range -85° to 0°) on a HEALPix² [10] grid corresponding to a resolution of about 0.5° . In a second iteration we zoom in on the most interesting regions. This search is not motivated by any prior knowledge regarding the position of the sources, instead we are limited by the large number of trials performed, which together with the angular resolution gives a limit on the effective number of individual points tested. The pre-trial p-values obtained are converted into post-trial p-values by counting the fraction of times we get an equal or greater pre-trial p-value from an ensemble of 10000 pseudo-experiments where the right ascension directions were scrambled, see figure 3.

We also perform a search at the position of 96 pre-defined sources: all 84 TeVCat³ [11] sources in the Southern Hemisphere (as of May 2015) and in addition 12 sources traditionally tested by IceCube ('GX 339-4', 'Cir X-1', 'PKS 0426-380', 'PKS 0537-441', 'QSO 2022-077', 'PKS 1406-076', 'PKS 0727-11', 'QSO 1730-130', 'PKS 0454-234', 'PKS 1622-297', 'PKS 1454-354', 'ESO 139-G12'). The TeVCat listing consists of sources seen by ground-based gamma-ray experiments, such as VERITAS, MAGIC, and H.E.S.S. and from these we consider sources from the catalogs 'Default Catalog' and 'Newly Announced', stable sources published or pending publication in refereed journals.

Figure 2 shows the median sensitivity of the LESE analysis for four different signal hypotheses as a function of declination. Further we illustrate the joint effort within the IceCube collaboration towards lowering the energy threshold for point source searches by showing the differential sensitivity for four different analyses: the LESE analysis, the STeVE (Starting TeV Events) analysis optimized at slightly higher energies (few TeV - 100 TeV) [12], and the classic through-going point

²<http://healpix.sourceforge.net>

³<http://tevcad.uchicago.edu>

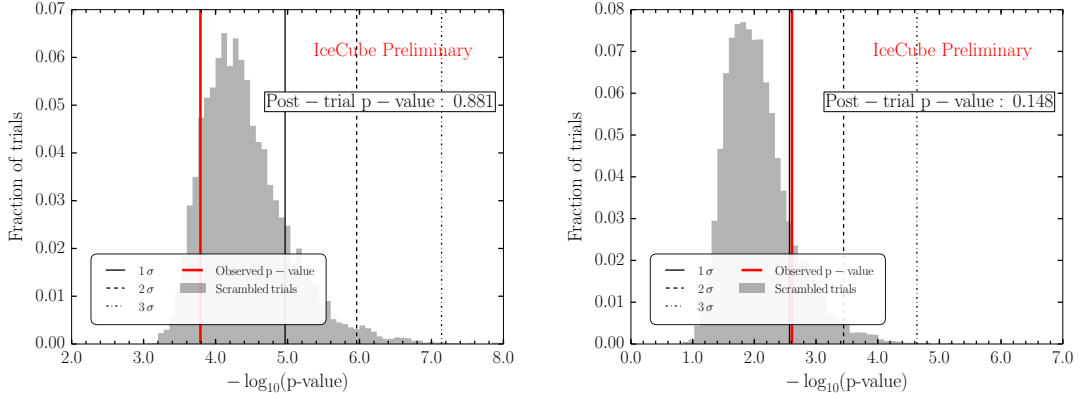


Figure 3: Pre-trial p-value distribution from 10000 scrambled trials for the sky scan (left) and the source list scan (right). The red line indicates the observed best p-values for the hottest spot and hottest source respectively, while the black vertical lines represent the 1, 2, and 3 σ significance levels.

source analysis in black [13]. The sensitivities shown correspond to 3 years of operation and were estimated by simulating events with the livetime corresponding to the MESE (Medium-Energy Starting Events) analysis focusing on energies in the region 100 TeV - 1 PeV [14].

5. Results

The pre-trial p-value distribution for the all sky search is shown in figure 4. The hottest spot is located at right ascension 305.2° and declination -8.5° with a pre-trial p-value of $1.6 \cdot 10^{-4}$ and a post-trial p-value of 88.1% (best fit parameters $\hat{n}_s = 18.3$ and $\hat{\gamma} = 3.5$). In figure 5 we show a zoom in on the \mathcal{TS} distribution in the area surrounding the hottest spot and further a zoom in on the individual event weights $\log(1 + n_s \chi_i)$ that contribute to the test statistic at the position and with the best fit parameters of the hottest spot.

The most significant source in the pre-defined list was QSO 2022-077⁴, a Flat-Spectrum Radio Quasar (FSRQ), with a pre-trial p-value of $2.5 \cdot 10^{-3}$. The post-trial p-value is 14.8%. For the sources in the list, we calculate the upper limit at 90% confidence level (C.L.) based on the classical approach [15] for the signal hypotheses: $d\Phi/dE_\nu \propto E_\nu^{-2}$, $E_\nu^{-2}e^{-E_\nu/10 \text{ TeV}}$, $E_\nu^{-2}e^{-E_\nu/1 \text{ TeV}}$, and E_ν^{-3} ,

Table 1: The most significant sources in the pre-defined list. The p-values are the pre-trial probability of being compatible with the background-only hypothesis. The \hat{n}_s and $\hat{\gamma}$ are the best-fit values from the likelihood optimization. We further show the flux upper limit Φ at 90% C.L. for a number of neutrino flux models. These are shown for the combined flux of ν_μ and $\bar{\nu}_\mu$ in units $\text{TeV}^{\gamma-1} \text{cm}^{-2} \text{s}^{-1}$.

Source	R.A. [°]	dec. [°]	$-\log_{10}(\text{p-val.})$	\hat{n}_s	$\hat{\gamma}$	$\Phi_{\nu_\mu + \bar{\nu}_\mu}^{90\%} \times \text{TeV}^{\gamma-1} \text{cm}^{-2} \text{s}^{-1}$			
						E_ν^{-2}	$E_\nu^{-2}e^{-E_\nu/10 \text{ TeV}}$	$E_\nu^{-2}e^{-E_\nu/1 \text{ TeV}}$	E_ν^{-3}
QSO 2022-077	306.5	-7.6	2.61	17.3	3.5	$6.74 \cdot 10^{-10}$	$5.81 \cdot 10^{-9}$	$1.56 \cdot 10^{-9}$	$1.27 \cdot 10^{-9}$
HESS J1718-385	259.5	-38.5	1.58	5.9	3.4	$7.62 \cdot 10^{-10}$	$3.21 \cdot 10^{-8}$	$2.80 \cdot 10^{-9}$	$5.58 \cdot 10^{-9}$
HESS J1841-055	280.3	-5.53	1.48	5.0	2.4	$5.01 \cdot 10^{-10}$	$4.52 \cdot 10^{-9}$	$1.19 \cdot 10^{-9}$	$9.88 \cdot 10^{-10}$
KUV 00311-1938	8.4	-19.4	1.40	7.1	3.4	$8.25 \cdot 10^{-10}$	$1.33 \cdot 10^{-8}$	$2.47 \cdot 10^{-9}$	$2.65 \cdot 10^{-9}$
30 Dor C	83.9	-69.1	1.04	2.3	3.6	$9.14 \cdot 10^{-10}$	$5.35 \cdot 10^{-8}$	$3.65 \cdot 10^{-9}$	$7.92 \cdot 10^{-9}$

⁴Alternate name: 2EG J2023-0836

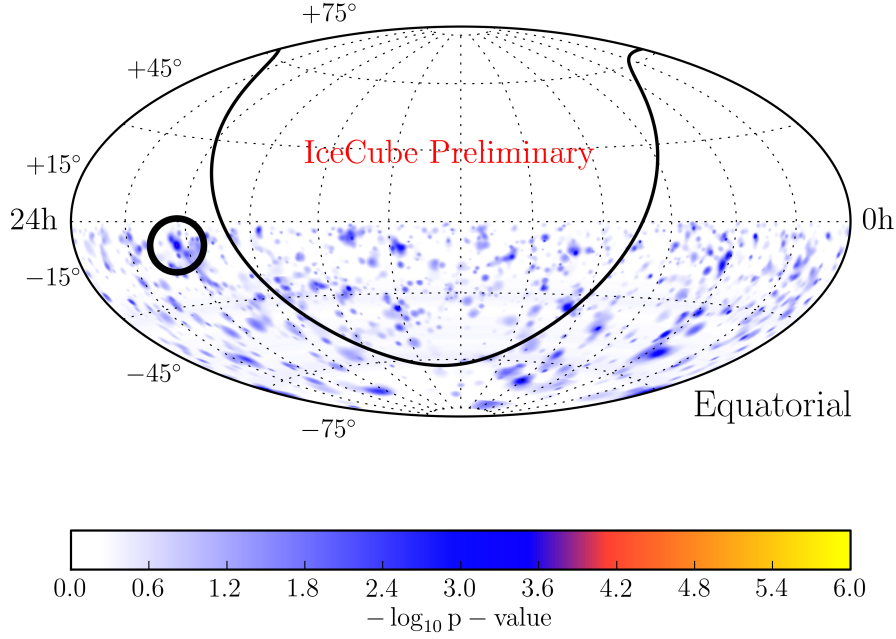


Figure 4: Pre-trial significance skymap in equatorial coordinates (J2000) showing the LESE analysis result on data from the first year of the full 86-string configuration of IceCube. The location of the Galactic plane is illustrated with a black solid line and the position of the most significant fluctuation is indicated with a black circle. The hottest spot is located at R.A. 305.2° and dec. -8.5° with a pre-trial p-value of $1.6 \cdot 10^{-4}$. The corresponding post-trial p-value is 88.1%.

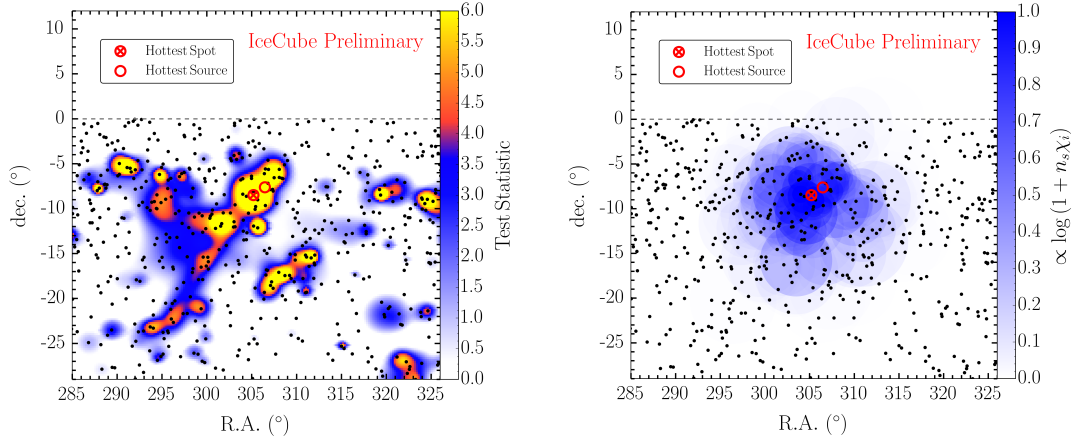


Figure 5: Zoom on the hottest spot (red circle + cross) and hottest source (red circle) in equatorial coordinates R.A. and dec. The reconstructed position of each event is shown in black dots. Left: The color transparency indicates the test statistic value at each pixel in the sky. Right: The radii of the circles are equal to the estimated angular uncertainty of each event. Color transparency indicate the strength of the individual likelihood weights $\log(1 + n_s \chi_i)$ that contribute to the test statistic at the position and with the best fit parameters of the hottest spot.

see figure 2. The limits of the five most significant sources are presented in table 1 along with the best fit parameters n_s and γ . Note that we do not consider under fluctuations, i.e. for observed values of \mathcal{TS} below the median of \mathcal{TS} for the background-only hypothesis we report the corresponding median upper limit.

6. Summary and Outlook

No evidence of neutrino emission from point-like sources in the Southern Hemisphere at low-energies (100 GeV - few TeV) was found in the first year of data from the 86-string configuration of IceCube. The most significant spot in the sky has a post-trial p-value of 88.1%. Further we tested the presence of signal from 96 sources in a pre-defined source list of known γ -ray emitters seen in ground-based telescopes. The results are consistent with the background-only hypothesis. The most significant source has a post-trial p-value of 14.8%. Upper limits at 90% C.L. were calculated for these sources for a number of signal hypotheses, see figure 2 and table 1.

Three more years of IceCube data with the full configuration exist and are ready to be incorporated into this analysis. We expect the sensitivity to improve slightly faster than the square-root of time limit, due to the relatively low background rate. Further, we have plans of performing a search for extended point sources and for neutrino emission in the Galactic plane.

References

- [1] W. Bednarek, G. F. Burgio, and T. Montaruli, *New Astron.Rev.* **49** (2005) 1.
- [2] A. Kappes, J. Hinton, C. Stegmann, and F. A. Aharonian, *Astrophys.J.* **656** (2007) 870.
- [3] M. D. Kistler and J. F. Beacom, *Phys.Rev.* **D74** (2006) 063007.
- [4] **IceCube** Collaboration, A. Achterberg et al., *Astropart.Phys.* **26** (2006) 155.
- [5] **IceCube** Collaboration, R. Abbasi et al., *Astropart.Phys.* **35** (2012) 615.
- [6] **IceCube** Collaboration, R. Abbasi et al., *Nucl.Instrum.Meth.* **A700** (2013) 188.
- [7] T. Neunhoffer, *Astropart.Phys.* **25** (2006) 220.
- [8] **IceCube** Collaboration, M. Aartsen et al., *JINST* **9** (2014) P03009.
- [9] J. Braun, J. Dumm, F. De Palma, C. Finley, A. Karle, et al., *Astropart.Phys.* **29** (2008) 299.
- [10] K. M. Górski, E. Hivon, A. J. Banday, B. D. Wandelt, F. K. Hansen, M. Reinecke, and M. Bartelmann, *The Astrophysical Journal* **622** (2005), no. 2 759.
- [11] S. P. Wakely and D. Horan, *TeVCat: An online catalog for Very High Energy Gamma-Ray Astronomy*, in *Proceedings, 30th International Cosmic Ray Conference (ICRC 2007)*, vol. 3, p. 1341, 2007.
- [12] **IceCube** Collaboration, M. Aartsen et al., *Medium-energy (few TeV - 100 TeV) neutrino point source searches in the Southern sky with IceCube*, in *PoS(ICRC2015)1056 these proceedings*, 2015.
- [13] **IceCube** Collaboration, M. Aartsen et al., *Searches for Extended and Point-like Neutrino Sources with Four Years of IceCube Data*, 2014. [arXiv:1406.6757](https://arxiv.org/abs/1406.6757).
- [14] J. Feintzeig, *Searches for Point-like Sources of Astrophysical Neutrinos with the IceCube Neutrino Observatory*. PhD thesis, University of Wisconsin, Madison, 2014.
- [15] J. Neyman, *Royal Society of London Philosophical Transactions Series A* **236** (1937) 333.

Medium-energy (few TeV - 100 TeV) neutrino point source searches in the Southern sky with IceCube

The IceCube Collaboration[†],

[†] http://icecube.wisc.edu/collaboration/authors/icrc15_icecube

E-mail: david.altmann@desy.de

Many galactic sources of gamma rays are suspected to also produce high-energy neutrinos with a typical high-energy cutoff below 100 TeV. At the location of IceCube, the Galactic Center and a large fraction of the Galactic Plane lie continuously above the horizon, where the large background of atmospheric muons makes any search for galactic neutrino sources extremely challenging. This background can be significantly reduced by using the outer portion of the detector as a veto and by applying event topology cuts. The data were taken during the first year of the completed IceCube detector and correspond to a livetime of 337 days. The event selection, optimized for neutrino energies between a few TeV and 100 TeV, is presented along with the results for a southern sky point source scan and the investigation of selected sources.

Corresponding authors: D. Altmann^{1,2*}, A. Kappes²,

¹ DESY, Platanenallee 8, 15378 Zeuthen, Germany

² ECAP, Physikalisches Institut, Erwin-Rommel-Straße 1, 91058 Erlangen, Germany

*The 34th International Cosmic Ray Conference,
30 July- 6 August, 2015
The Hague, The Netherlands*

*Speaker.

1. Introduction

The southern sky provides a large variety of interesting objects for a search of point-like sources of astrophysical neutrinos, such as the galactic center and numerous other potential neutrino sources [1, 2, 3, 4]. Gamma-ray spectra observed by FERMI or HESS suggest some of these objects produce gamma rays by hadronic mechanisms[5]. However, for most of them the separation between hadronic or leptonic production is not obvious. The detection of neutrinos from these sources with IceCube would provide us with a better understanding of the source environment.

IceCube is a cubic-kilometer neutrino detector installed in the ice at the geographic South Pole [6] between depths of 1450 m and 2450 m. Detector construction started in 2005 and finished in 2010. Neutrino reconstruction relies on the optical detection of Cerenkov radiation emitted by secondary particles produced in neutrino interactions in the surrounding ice or the nearby bedrock.

Traditionally, the ν_μ charged-current channel is the preferred signal, since the muons produced leave a track-like pattern in the detector. This pattern can be reconstructed with good angular precision (for most energies better than two degrees). Thus, the reconstructed direction of the muon points back to the source of the neutrino. However, in the southern sky this scheme is challenging due to the large background of muons produced in the atmosphere. In recent years, several IceCube searches [7, 8, 9] which select neutrino events interacting inside the detector volume (so called "starting" events), proved to be very successful – most known for the detection of the high-energy astrophysical neutrino flux [8].

This contribution presents a new selection of data taken during the first year of operation of the completed IceCube detector. The selection discussed in this paper is optimized for the detection of "starting" events from interactions of ν_μ with energies between a few TeV and 100 TeV (called in what follows STeVE, Starting TeV Events). An analysis concentrating on lower energies (below few TeV), Low-Energy Starting Event (LESE) is discussed in [10], and an analysis focusing on Medium-Energy (100 TeV - 1 PeV) Starting Events (MESE) has been presented in [11].

2. Data selection

The main challenge for the STeVE analysis is the vast background of muons. A very successful way to separate these muons from neutrinos is the selection of starting tracks. A starting track is an event where a neutrino interacts within the detector volume and produces a muon. The hadronic cascade at the interaction vertex and the muon create a hit pattern that does not start at the edges of the detector, but somewhere inside the detector volume. In principle such a pattern can only be produced by a neutrino. However, due to the relatively large string separation of IceCube, 125 m, atmospheric muons can pass through the outer layers of the detector and mimic a hit pattern that is very similar to that of a starting event neutrino interaction.

A first selection step is the implementation of an event filter that is optimized to keep as many starting events as possible while rejecting over 90 percent of the atmospheric muons, reducing the event rate from about 2200 events per second at trigger level to about 190 events per second. For this, the starting vertex of the event is reconstructed if the event passes a pre-selection, based on the position and type of the hit pattern in the detector (see [10] for more detail on the pre-selection

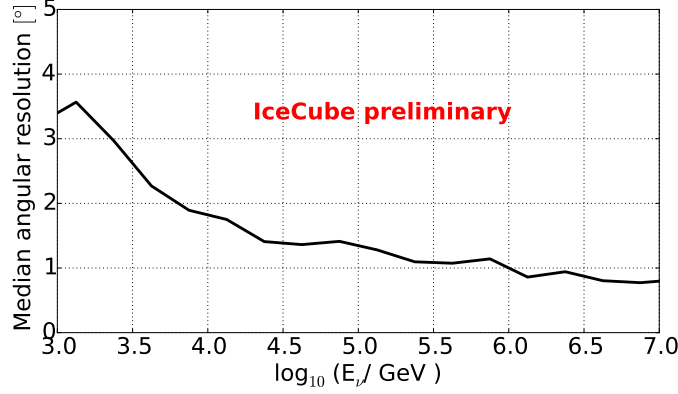


Figure 1: Median angular resolution of simulated muon neutrinos in the event sample plotted as a function of true neutrino energy.

and [12] for details on the reconstruction algorithm). If the vertex is within the contained volume, the event is kept. After this initial step, the data selection of the LESE and STeVE analyses differ.

The usage of advanced reconstruction methods is computationally expensive. Therefore, the event sample is reduced by an energy cut to a rate of about 7 events/s. For this reduced sample, the direction is reconstructed again with a more accurate algorithm using the multiple photoelectron PDF [13] that describes the arrival time of the first of multiple photons. Since the optical properties of the glacial ice at the South Pole are not uniform with depth, we calculate these PDFs with a Monte-Carlo using a realistic ice model [14] and then fit the PDFs with splines [15]. Then the stochastic energy losses along the reconstructed track are calculated using the unfolding algorithm discussed in [16].

The stochastic energy loss pattern provided by the unfolding is then used to calculate several variables based on the energy and length of the event, like the initial energy deposition of the track or the depth inside the detector of the initial energy deposition. With these and other track reconstruction variables, a Boosted Decision Tree (BDT) is trained. The final cut on the BDT score is then optimized to provide the optimal sensitivity for a point-like source search. During data taking operation, the IceCube detector can run with incomplete configurations of strings. Though these runs are rare, they can be problematic for an event selection that uses the event topology as a main selection criterion; therefore, they are excluded, reducing the livetime by about 30 days.

At final level, the event sample consists of 10178 events. Most of these events are expected to be remaining atmospheric muons. The number of background events is reduced by a factor of about 10^7 . Roughly 20 percent of all starting muon tracks from neutrino interactions within the detector volume and $E_\nu > 10 \text{ TeV}$ are kept. The median angular resolution is shown in Fig. 1. Compared to other point source searches [17], the resolution is somewhat worse, mainly due to the shorter length of the events compared to a through-going event sample. The effective area of this analysis at final cut level is shown in Fig. 2.

3. Analysis method

To calculate the probability that an excess of events at a certain position is due to a fluctuation

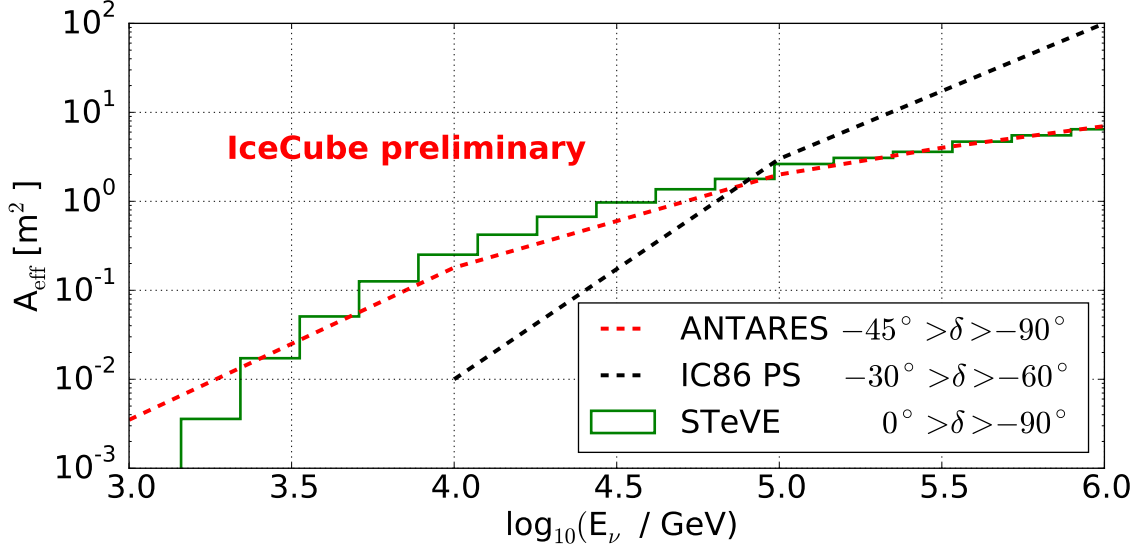


Figure 2: Effective area of the STeVE analysis compared to the IC86 through-going PS analysis (marked as IC86 PS) [17] and ANTARES [18]. δ is the declination of the neutrino event.

of the background, an unbinned maximum likelihood method [19] is used. For a given event and location in the sky, we compute the PDFs S_i and B_i describing the compatibility of the event with the signal and background hypotheses, respectively. These PDFs depend on the event energy and the angular difference between the reconstructed event direction and the location in the sky. The shape of the signal pdf depends on the spectral index γ and, in some investigated scenarios, on the cutoff in energy. The PDF, $f(n_s)$, describing the event under the combined signal and background hypothesis, is given in equation 3.1, where N is the number of events in the sample and n_s is a free parameter to select the relative weight of the signal and background PDFs. For the entire data set, the product of the single event probabilities defines the likelihood (\mathcal{L}), shown in eq. 3.2. For a hypothetical point source location, \mathcal{L} is maximized over the data set with respect to n_s and signal spectral index (γ), giving the best-fit values \hat{n}_s and $\hat{\gamma}$. The signal hypothesis is compared to the background hypothesis of no signal ($n_s = 0$). The ratio of both hypotheses yields the test statistic (TS) shown in eq. 3.3.

$$f(n_s) = \frac{n_s}{N} S_i + \left(1 - \frac{n_s}{N}\right) B_i \quad (3.1)$$

$$\mathcal{L}(n_s) = \prod_i^N [f(n_s)] \quad (3.2)$$

$$\text{TS} = -2 \log \left(\frac{\mathcal{L}(n_s = 0)}{\mathcal{L}(\hat{n}_s, \hat{\gamma})} \right) \quad (3.3)$$

The distribution of the TS for the null-hypothesis is assessed by generating a few thousand pseudo-experiments, which are created by scrambling the events in right ascension. Then for each of the scrambled skies, the TS at the investigated point is calculated. These TS distributions can differ for different zenith bands. Therefore, the zenith-independent p-value = $\eta \cdot \chi^2(ndof, TS)$ is

Source	\hat{n}_s	$\hat{\gamma}$	p-value	$\Phi_{\nu_\mu + \bar{\nu}_\mu}^{90\%} \times 10^{-12} \text{ TeV}^{-1} \text{ cm}^{-2} \text{ s}^{-1}$		
				No E_{cut}	$E_{\text{cut}} = 100 \text{ TeV}$	$E_{\text{cut}} = 10 \text{ TeV}$
HESS J1458-608	3.96	2.6	79.2 %	203	432	6506
HESS J1837-069	5.18	3.2	85.7 %	175	258	1172
SNR G000.9+00.1	8.14	4.0	35.4 %	295	560	3659
Terzan 5	3.41	2.9	98.9 %	231	414	2952
HESS J1507-622	4.09	2.7	85.9 %	203	423	6813
HESS J1841-055	4.77	3.3	91.3 %	159	236	909

Table 1: Table of all sources with post trial background probability smaller than 100%. Listed are the signalness parameter \hat{n}_s , the fitted spectral index $\hat{\gamma}$, the calculated background probability after trial-correction and the upper limit on the flux for an E^{-2} spectrum without a cutoff and two scenarios with a hard cutoff in units of $10^{-12} \text{ TeV}^{-1} \text{ cm}^{-2} \text{ s}^{-1}$.

used. Here η is the correction factor for the $\text{TS}=0$ values, caused by the restriction to a positive signal-parameter n_s , and $ndof$ is the number of effective degrees of freedom, computed by a fit of a χ^2 function to the tail of the TS distribution. Based on these TS distributions one can calculate how likely a certain value is. If one does not look at a single point in the sky, but a few (like in a source list) or many (like in an all-sky scan), the trial factor has to be considered. For this, again, we use scrambled skies and then calculate, for the entire investigated ensemble of points, the distribution of maximal $-\log_{10}(\text{p-value})$. Based on this distribution the probability to measure a source that is at least as unlikely as the measured one can be calculated.

We used two approaches to search for potential point-like sources:

3.1 Source list

The source list is mainly based on TeVCat sources [20]. Here, all sources in the southern sky (84) are selected. Additionally, 12 source candidates that were under investigation in previous IceCube searches for point-like sources (see [17]) but are not in the TeVCat are added.

Of the 96 investigated sources, none showed a significant over-fluctuation after correcting for trial factors. SNR G000.9+00.1 is the source with the smallest background probability of 0.5% before trial correction. After trial correction this source has a background probability of 35.4%. The six sources with the lowest background probability are shown in Table 1. Upper limits were calculated using the Neyman method [21]. The sensitivity, discovery potential and upper limits for the investigated sources, assuming a scenario with an E^{-2} dependence on neutrino energy with a cutoff of 100 TeV, are shown in Fig. 3.

3.2 Southern sky scan

Additionally, we scanned the southern sky with a HEALPix¹ [23] grid with a bin width of about 0.46 degree. This is well below the angular resolution of the sample (as shown in Fig 1). For each point, the background probability was calculated in the same way as for the source list, resulting in the skymap shown in Fig. 4. The point with the lowest background probability is found at right ascension 93.1° , declination -64.3° . Correcting for the trial factor yields a probability of

¹<http://healpix.sourceforge.net>

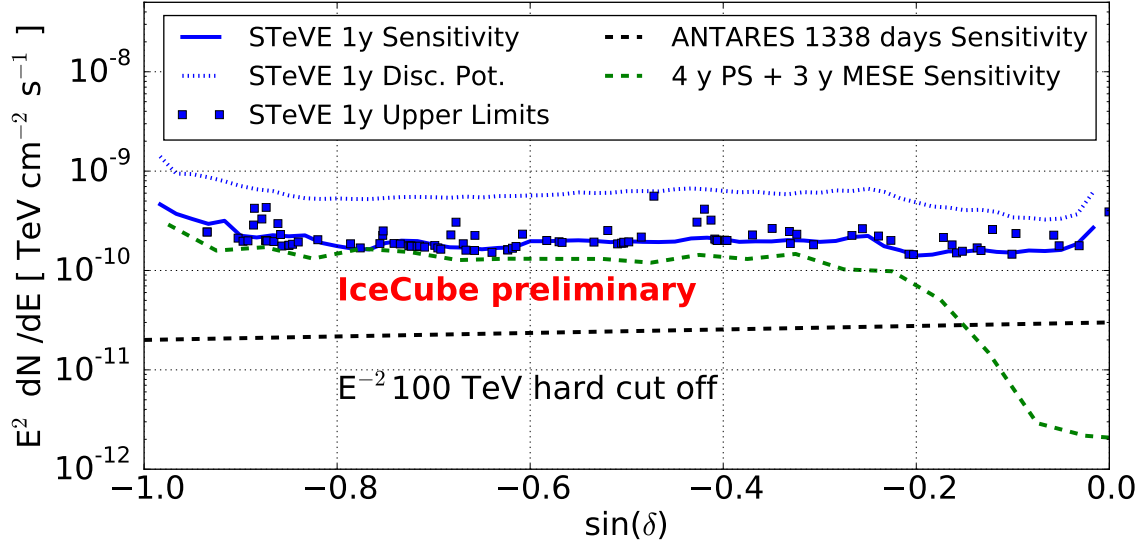


Figure 3: Sensitivities for STeVE (solid line), ANTARES [22] and the combined MESE [11] and through-going IceCube point-like source search [17] (dashed lines) with their respective livetimes. Additionally, the discovery potential (dotted) and upper-limits on the investigated sources for the STeVE analysis (squares) are shown. The assumed spectrum is E^{-2} with a hard cutoff at 100 TeV.

74.9% that a background fluctuation at least as significant happened anywhere in the observed sky during the observation time. Thus, the results of the sky scan are fully compatible with the background-only hypothesis.

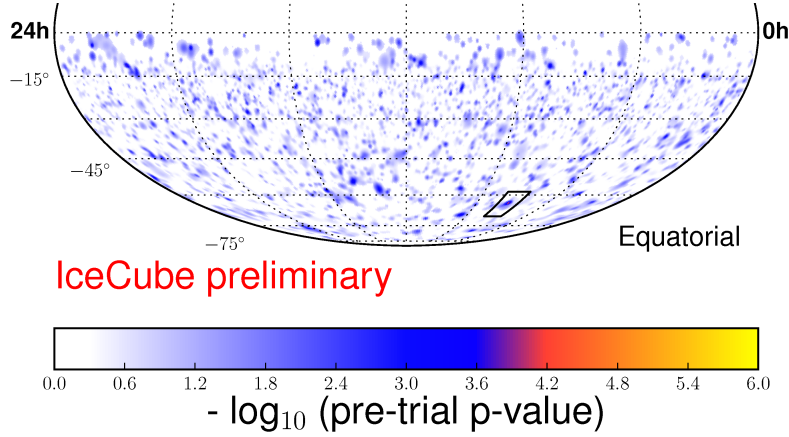


Figure 4: Fitted p-values in the southern sky. The point with the lowest background probability is found at right ascension 93.1° , declination -64.3° (in the center of the black rectangle).

4. Conclusions

The STeVE analysis has not found any indication for a point-like source of neutrino emission in the southern sky using data corresponding to 337 days of detector livetime. For the energy

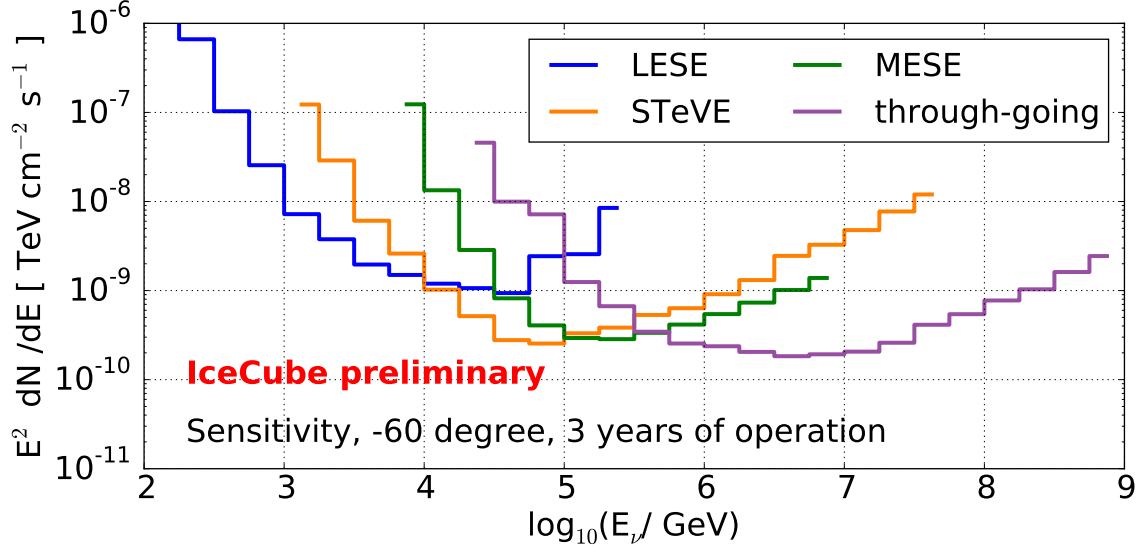


Figure 5: The differential sensitivities for four IceCube point-like source searches in the southern sky. The sensitivities for LESE [10], STeVE and the through-going analysis [17] are estimated simulating events with a livetime of MESE [11].

region of interest below 100 TeV, the 90% C.L. upper limits are competitive with other IceCube results. This could be achieved with a livetime of one year compared to the combined three year MESE / four year through-going IceCube point-like source search. However, due to worse angular resolution and higher number of background events, the presented limits are not yet very competitive with the limits of the searches with ANTARES [22]. A combination of LESE/STeVE/MESE and through-going IceCube point-like source searches would cover an unprecedented energy range from a few 100 GeV to EeV (see Fig. 5).

References

- [1] A. Kappes, J. Hinton, C. Stegmann, and F. A. Aharonian, *Astrophys.J.* **656** (2007), no. 2 870.
- [2] M. D. Kistler and J. F. Beacom, *Phys.Rev.* **D74** (2006) 063007, [[astro-ph/0607082](#)].
- [3] F. Vissani and F. Aharonian, *Nucl.Instrum.Meth.* **A692** (Nov., 2012) 5–12, [[arXiv:1112.3911](#)].
- [4] Q. Yuan, P.-F. Yin, and X.-J. Bi, *Astropart.Phys.* **35** (Aug., 2011) 33–38, [[arXiv:1010.1901](#)].
- [5] **Fermi-LAT** Collaboration, M. Ackermann et al., *Science* **339** (2013) 807, [[arXiv:1302.3307](#)].
- [6] **IceCube** Collaboration, A. Achterberg et al., *Astropart.Phys.* **26** (2006), no. 3 155 – 173.
- [7] **IceCube** Collaboration, M. Aartsen et al., *Science* **342** (2013) 1242856, [[arXiv:1311.5238](#)].
- [8] **IceCube** Collaboration, M. Aartsen et al., *Phys.Rev.* **D91** (2015), no. 2 022001, [[arXiv:1410.1749](#)].
- [9] **IceCube** Collaboration, M. Aartsen et al., *Phys.Rev.Lett.* **113** (2014) 101101, [[arXiv:1405.5303](#)].
- [10] **IceCube** Collaboration, M. Aartsen et al., *Low-energy (100 GeV - few TeV) neutrino point source searches in the Southern sky with IceCube*, in *PoS(ICRC2015)1053, these proceedings*, 2015.

- [11] J. Feintzeig, *Searches for Point-like Sources of Astrophysical Neutrinos with the IceCube Neutrino Observatory*. PhD thesis, University of Wisconsin, Madison, 2014.
- [12] S. Euler, *Observation of oscillations of atmospheric neutrinos with the IceCube Neutrino Observatory*. PhD thesis, RWTH Aachen, 2014.
- [13] **AMANDA** Collaboration, J. Ahrens et al., *Nucl.Instrum.Meth.* **A524** (2004) 169–194, [[astro-ph/0407044](#)].
- [14] **IceCube** Collaboration, M. Aartsen et al., *Nucl.Instrum.Meth.* **A711** (2013) 73–89, [[arXiv:1301.5361](#)].
- [15] N. Whitehorn, J. van Santen, and S. Lafebre, *Comput.Phys.Commun.* **184** (2013) 2214–2220, [[arXiv:1301.2184](#)].
- [16] **IceCube** Collaboration, M. Aartsen et al., *JINST* **9** (2014) P03009, [[arXiv:1311.4767](#)].
- [17] **IceCube** Collaboration, M. Aartsen et al., *Astrophys.J.* **796** (2014), no. 2 109, [[arXiv:1406.6757](#)].
- [18] **ANTARES** Collaboration, S. Adrian-Martinez et al., *Astrophys.J.* **760** (2012) 53, [[arXiv:1207.3105](#)].
- [19] J. Braun, J. Dumm, F. De Palma, C. Finley, A. Karle, et al., *Astropart.Phys.* **29** (2008) 299–305, [[arXiv:0801.1604](#)].
- [20] S. Wakely and D. Horan, *TeVCat: An online catalog for Very High Energy Gamma-Ray Astronomy*, in *Proc. of the International Cosmic Ray Conference*, vol. 3, pp. 1341–1344, 2007.
- [21] J. Neyman, *Philosophical Transactions of the Royal Society of London A: Mathematical, Physical and Engineering Sciences* **236** (1937), no. 767 333–380.
- [22] **ANTARES** Collaboration, S. Adrian-Martinez et al., *Astrophys.J.* **786** (2014) L5, [[arXiv:1402.6182](#)].
- [23] K. M. Górski, E. Hivon, A. J. Banday, et al., *Astrophys.J.* **622** (Apr., 2005) 759–771, [[astro-ph/0409513](#)].

The Online Follow-Up Framework for Neutrino Triggered Alerts from IceCube

The IceCube Collaboration¹

[†] http://icecube.wisc.edu/collaboration/authors/icrc15_icecube

E-mail: alexander.stasik@desy.de

The current operation of online programs for sending follow-up alerts to optical, X-ray and gamma-ray telescopes shows the feasibility of neutrino-triggered multi-messenger astronomy. Building on the experience of these programs, we generalize the approach and merge them into a combined generic framework. The upgrade consists of a single event stream selected at the South Pole and transmitted north, where an online search for transients and flaring points is performed. The event selection will be compared to established offline point source searches in IceCube. Performance of the stream in terms of delay and stability will be shown.

Corresponding authors: Alexander Johannes Stasik^{1*}, Thomas Kintscher¹, Marek Kowalski^{1,2}, Elisa Bernadini^{1,2}

¹ *Deutsches Elektronen-Synchrotron (DESY), Platanenallee 6, D-15735 Zeuthen, Germany*

² *Institut für Physik, Humboldt Universität, Newtonstr. 15, D-12489 Berlin, Germany*

*The 34th International Cosmic Ray Conference,
30 July- 6 August, 2015
The Hague, The Netherlands*

*Speaker.

1. Introduction

Neutrinos play an important role in modern astrophysics due to their complementary nature to other messengers like photons and cosmic rays [1]. Neutrinos only interact through the weak force making them a natural choice for astronomy since they are neither deflected by magnetic fields nor absorbed between source and observer and thus point back to their origin. The production of high energetic neutrinos is associated with hadronic interactions and thus is directly linked to cosmic rays. This makes neutrinos a viable tool to search for sources of the highest energy cosmic rays. However, detection of astrophysical neutrinos is very challenging due to their small cross section and the large background of atmospheric muons and atmospheric neutrinos.

While the angular resolution of neutrino telescopes is orders of magnitude worse than modern optical telescopes, they have a field of view that can cover the entire sky with a duty cycle of almost 100%. This complementary nature of neutrino telescopes and typical electromagnetic telescopes motivates the combination of these channels. IceCube has shown the existence of astrophysical neutrinos, but no sources have yet been identified [2, 3].

While for steady sources combining different messenger channels like neutrino and electromagnetic data is possible with archival data, transient sources benefit strongly from real time follow-up observation with small field-of-view optical telescopes. Thus external real time triggers are required. IceCube with its all-sky field-of-view can provide such triggers. The typical time scales of potential sources vary between several hundred days for supernovae or flaring AGNs [4] and go down to several seconds for short GRBs [5]. These Neutrino triggered Target of Opportunity (NToO) programs require highly automated and stable systems since the entire analysis, from identifying an interesting event to notifying follow-up observatories and changing observation schedules, has to be done in seconds and possibly even without a human being involved in the loop.

IceCube plays a central role as a triggering facility in many multi-messenger efforts. Different follow-up programs like optical (OFU) [6], X-ray follow-up (XFU) [7] and gamma follow-up (GFU) [8] have been independently running for several years [9]. Under these programs, alerts have been sent to PTF [10], the Swift satellite [11], MAGIC [12], Veritas [13] and the multi-messenger network AMON [14]. These systems analyze the neutrino data in real time at the South Pole. Only follow-up alerts leave the Pole in real-time while the sub-threshold data stays at the detector and is only available for offline studies. This paper describes the design and capabilities of the new IceCube real time system. The new system provides for the first time a stream of high quality events in real time available in the north with a latency of a few tens of seconds. This sub-threshold stream offers many new opportunities in multi-messenger astronomy [14]. Section 2 will describe the IceCube neutrino telescope. Section 3 will present the design behind the real time system running in IceCube. Section 4 will show the sensitivity for the event selections available in near real time in the current system.

2. The IceCube Neutrino Telescope

IceCube is a cubic-kilometer neutrino detector installed in the ice at the geographic South Pole between depths of 1450 m and 2450 m. Detector construction started in 2005 and finished in

2010. Neutrino reconstruction relies on the optical detection of Cherenkov radiation emitted by secondary particles produced in neutrino interactions in the surrounding ice or the nearby bedrock [15]. Neutrinos can interact and produce secondary particles via charged current (CC) or neutral current (NC) interactions. While NC interactions produce a localized hadronic cascade inside the ice, CC interactions produce an additional lepton corresponding to the initial neutrino flavor. Electrons and tau leptons typically lose their energy on length scales of several meters, normally indistinguishable from the hadronic cascade. NC and CC neutrino interactions caused by electron or tau neutrinos produce localized, almost spherical signatures inside the detector. These event signatures are called cascades. While their directional reconstruction is challenging due to their almost spherical shape, energy estimation is robust as long as the cascade is contained inside the detector, enabling a calorimetric measurement. Muons produced in ν_μ CC interactions, on the other hand, can travel many kilometers in ice and produce light along their way. These events are called tracks and provide good angular reconstructions at about one degree [16]. The track length can exceed the detector boundary, thus energy reconstructions are challenging since only the deposited energy inside the detector can be measured. At the neutrino energy of interest, the small kinematic angle between muon neutrino and muon is below the detector resolution and can be neglected [17]. Since track events are better suited for neutrino astronomy than cascades due to their better angular resolution, the following discussion is limited to ν_μ CC events.

Event selection starts from the online muon filter selection that identifies high quality tracks with a rate of about 40 Hz. This rate is dominated by atmospheric muons. To increase the neutrino purity of the sample, more advanced and more time consuming reconstructions are required. Since computing power is limited at the South Pole, these reconstructions can only be applied to a subset of the events. The *Online Level 2 Filter* uses the outcome of a likelihood reconstruction to further reduce the contamination from atmospheric muons. This likelihood reconstruction takes into account the actual photon propagation to the optical modules in the detector. Selection criteria are then, e.g., quality of the likelihood fit and the total number of modules detecting photons. After application of these criteria, the event rate is reduced to 5 Hz. More time-consuming reconstructions are applied afterwards, using a more advanced model for light propagation in the ice. They also explore the likelihood space to give an error on the angular reconstruction. Based on these reconstructions, a multivariate classifier is used for the final filter. At the end, the event rate is several mHz and has a neutrino purity of about 90%.

3. Online System

The goal of the IceCube real time system is to provide a system that can generate follow-up notifications called alerts with a minimal delay after one or more neutrinos are detected. The rate of false alerts should be as low as possible without losing signal events in the process. Also required are high stability and reliability since the entire system must run autonomously. Based on the event selection described in Section 2 a system has been built to transmit these events to the north, analyze them in real time and generate follow-up alerts to be send to other telescopes. The events are also used by IceCube for, e.g., real time event displays for detector monitoring purposes. The online system can handle any kind of event stream that is generated in real time at the Pole,

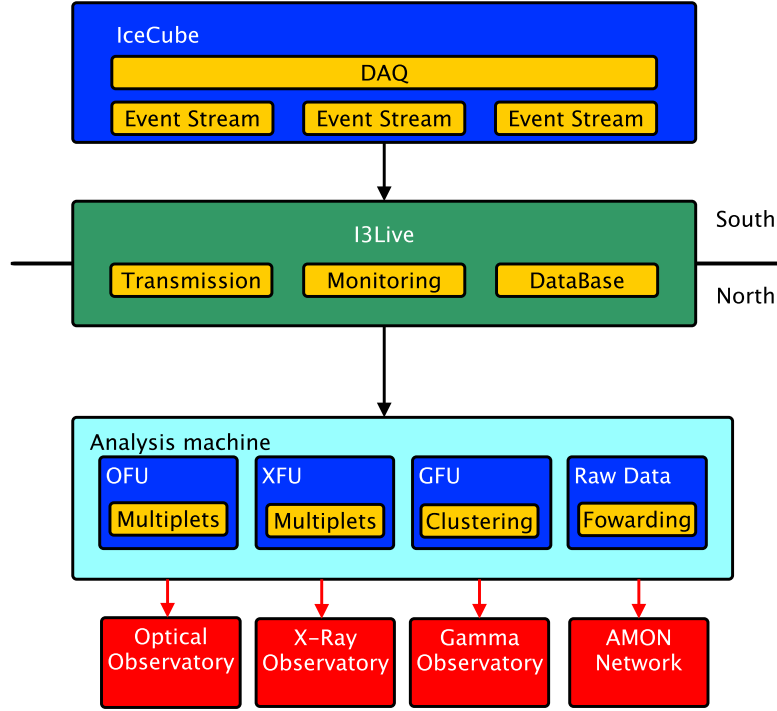


Figure 1: Sketch of the IceCube real time system. Black arrows indicate flow of event information and red arrows flow of alert information.

but since tracks from ν_μ CC events are the starting point of current online systems, discussion will focus here on this stream.

Once an event passes the filtering process described in Section 2, the full event information is stored on disk at the Pole. For data transmission to the north, IceCube uses several high bandwidth satellites which can transfer up to 100 GB per day. Due to the remote location of IceCube, these satellites are only available a few hours per day and thus are not suited for real time operations. To control and monitor the detector in real time, IceCube uses the *I3Live* system. *I3Live* has an instance running at South Pole and a mirrored version in the north. Both communicate using the Iridium satellite network [18]. Iridium satellites have a low bandwidth, but are available 24/7 with a latency of several seconds. The *I3Live* system at the South Pole is constantly listening to the stream of events exiting the filtering and processing system. If an event is marked as to have passed the real time event selection, it is picked up by *I3Live* and transmitted to the north. Due to bandwidth limitations it is not possible to transmit the entire event information, so just event direction, error estimator, energy estimator, event time and reconstruction quality parameters are sent north.

As the events arrive in the north, they are stored in a data base and forwarded to a dedicated machine that hosts the real time system in the north. This system consists of a set of follow-up clients each of which is dedicated to a specific set of events, a certain analysis method and a special follow-up facility to which it sends alerts. A software package is provided that includes generic functionality like interacting with the *I3Live* database, stability and monitoring tools for the client and tools like coordinate transformations and filter functions. Since every follow-up client will need

this functionality, the toolbox provided makes it easy to write a new client without knowledge of the technical side of the system. Figure 1 shows a sketch of the full python-based system. The system is modular so that additional channels (like e.g. the high energy starting event selection HESE [19] in real time) can just be added if they meet the computational and bandwidth requirements. It is also possible to simply add additional follow-up clients.

The transmission of single events has been since the beginning of this year. The delay is of the order of several seconds with some single outliers due to satellite connection problems. Figure 3 shows that the median delay is about 22 s and after 30 s about 99% of the events arrived.

4. Event selection

The main channel for triggering follow-up operations are ν_μ CC muon tracks due to their superior angular resolution. As described in Section 2, the muon track event selection has a final rate of about 5 mHz. Figure 2 shows the time-independent point source sensitivity of one year data processed as in the real time event stream to a data-set processed with offline algorithms. The offline data-set shows slightly better performance than the real time stream. This is a result of better, but much more time consuming, event reconstructions. The real time data, which is nearly as good as the offline data, can be processed in real time, decreasing latency from days to seconds.

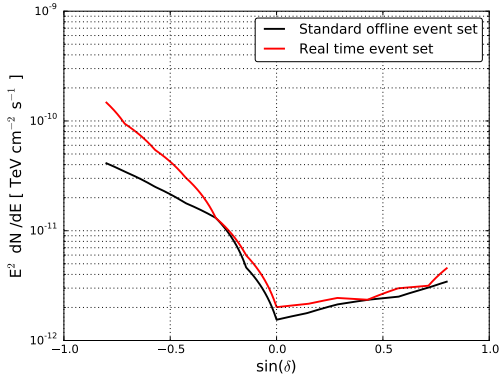


Figure 2: Time independent point source sensitivities for the online data stream compared to an offline event selection, 322 days livetime [20].

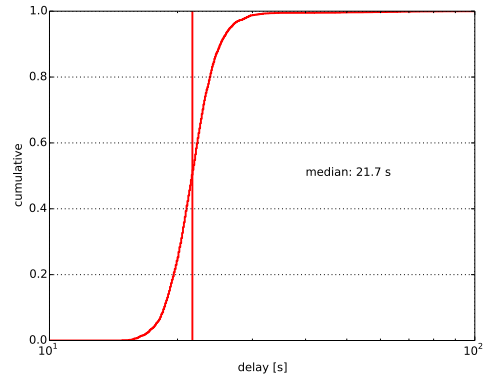


Figure 3: Cumulative distribution of delays between triggering time of the event and arrival time in the north.

5. Summary and outlook

The IceCube real time system provides a framework to process, transmit and analyze neutrino events with a typical latency of 20 to 30 seconds. The system is modular so that additional follow-up clients or event selections can be added if they can be filtered and reconstructed in real time at the Pole. The current implementation included high quality track like event stream. The point source sensitivity is slightly below the comparable offline data-set as expected due to computational limitations in real time.

References

- [1] T. K. Gaisser and T. Stanev, *Astroparticle Physics* **39** (Dec., 2012) 120–128, [[arXiv:1202.0310](#)].
- [2] **IceCube** Collaboration, M. Aartsen et al., *Science* **342** (2013) 1242856, [[arXiv:1311.5238](#)].
- [3] M. Kowalski, *ArXiv e-prints* (Nov., 2014) [[arXiv:1411.4385](#)].
- [4] A. M. Atoyan and C. Dermer, *New Astron.Rev.* **48** (2004) 381–386, [[astro-ph/0402646](#)].
- [5] E. Waxman and J. Bahcall, *Phys. Rev. Lett.* **78** (Mar, 1997) 2292–2295.
- [6] **IceCube, ROTSE** Collaboration, R. Abbasi et al., *Astron.Astrophys.* **539** (2012) A60, [[arXiv:1111.7030](#)].
- [7] P. Evans, J. Osborne, J. Kennea, M. Smith, D. Palmer, et al., *Mon.Not.Roy.Astron.Soc.* **448** (2015), no. 3 2210–2223, [[arXiv:1501.04435](#)].
- [8] **IceCube** Collaboration, M. Aartsen et al., [arXiv:1309.6979](#).
- [9] **IceCube** Collaboration, *PoS(ICRC2015)1052, these proceedings* (2015).
- [10] N. M. Law et al., *PASP* **121** (Dec., 2009) 1395–1408, [[arXiv:0906.5350](#)].
- [11] N. Gehrels et al., *Astrophysical Journal* **611** (Aug., 2004) 1005–1020.
- [12] C. Baixeras, *Nuclear Physics B - Proceedings Supplements* **114** (2003), no. 0 247 – 252. Proceedings of the XXXth International Meeting of Fundamentals Physics.
- [13] T. C. Weekes et al., *Astroparticle Physics* **17** (May, 2002) 221–243, [[astro-ph/0108478](#)].
- [14] **AMON** Collaboration, M. W. E. Smith et al., *Astroparticle Physics* **45** (May, 2013) 56–70, [[arXiv:1211.5602](#)].
- [15] **IceCube** Collaboration, A. Achterberg et al., *Astropart.Phys.* **26** (2006) 155–173, [[astro-ph/0604450](#)].
- [16] **IceCube** Collaboration, M. G. Aartsen et al., *Nuclear Instruments and Methods in Physics Research A* **736** (Feb., 2014) 143–149, [[arXiv:1308.5501](#)].
- [17] **ANTARES** Collaboration, , *ArXiv Astrophysics e-prints* (July, 1999) [[astro-ph/9907432](#)].
- [18] *Iridium communications inc.*, [www.iridium.com](#).
- [19] **IceCube** Collaboration, IceCube Collaboration, *Science* **342** (Nov., 2013) 1, [[arXiv:1311.5238](#)].
- [20] **IceCube** Collaboration, M. Aartsen et al., [arXiv:1406.6757](#).

Near Realtime Searches for Neutrinos from GRBs with IceCube

The IceCube Collaboration[†],

[†] http://icecube.wisc.edu/collaboration/authors/icrc15_icecube

E-mail: jfelde@icecube.umd.edu

Gamma Ray Bursts (GRBs) have long been suspected as the sources for the ultra high-energy cosmic rays. For this to be true, a mechanism must exist within the GRB to produce hadrons, a consequence of which is the production of neutrinos. So far, no significant observation has been made that suggests GRBs produce neutrinos. The IceCube neutrino Observatory, a cubic kilometer ice Cherenkov detector at the South Pole has put stringent limits on the theoretical models predicting prompt GRB neutrino and cosmic ray production. Although no significant observation has yet been made, even a single high-energy neutrino event coincident in time and direction to a known GRB could constitute a discovery. As such, we have implemented a rapid data processing and analysis scheme that allows for detection of possible GRB coincident neutrino events, as well as for the ability to send alerts of such events to other observatories for follow up observations. In this poster we describe the data processing and analysis scheme, the sensitivity of current searches, and the mechanism in place to send alerts for future IceCube observations.

Corresponding authors: J. Felde^{*1}

¹ *University of Maryland, College Park, MD 20742-4111*

*The 34th International Cosmic Ray Conference,
30 July- 6 August, 2015
The Hague, The Netherlands*

^{*}Speaker.

1. Introduction

Gamma Ray Bursts (GRBs) are known astrophysical phenomena that release a tremendous amount of energy, approximately $10^{51} - 10^{54} \text{ erg} \times \Omega/4\pi$, where Ω is the solid angle of a possible beamed emission, in a short amount of time, usually less than a couple of minutes [1]. Due to the extreme energy available, the possibility that GRBs are the sources of ultra high-energy cosmic rays (UHECRs) with energies above 10^{18} eV seems plausible, assuming a mechanism exists within the GRB acceleration engine to accelerate protons with a similar efficiency as electrons. Since the protons are charged, their trajectories will be altered by galactic and intergalactic magnetic fields, ruining any space and time correlation to their source. The presence of protons in the acceleration engine would give rise to interactions such as $p + \gamma \rightarrow \Delta^+ \rightarrow n + \pi^+$, where the pion would subsequently decay producing muon and electron neutrinos. Neutrinos are neutral, fundamental particles that are only weakly interacting, and as such, are capable of propagating over cosmic distances undeflected. If neutrinos are detected in spatial and temporal correlation with a known GRB, it would confirm the existence of high-energy proton acceleration in GRBs, supporting the hypothesis that GRBs produce the observed UHECRs.

In 2013, IceCube announced a discovery of high-energy neutrinos, above 10 TeV, of extraterrestrial origin, but no sources have been identified so far [2]. A recent search for neutrinos on time and on source from known GRBs during three years of IceCube construction (40, 59, and 79 strings) and one year with the completed (86 string) detector showed no significant correlation and is able to place tight limits on prompt neutrino production from GRBs. We conclude that no more than about 1% of the measured astrophysical flux may be attributed to prompt emission from known GRBs. Furthermore, tight limits can be placed on models that predict neutrino fluxes from GRBs; these results will be discussed in section 7. Although it does not appear that GRBs are ultimately responsible for the UHECRs, neutrinos may still be produced by GRBs. Moving forward, IceCube plans to automate previous analyses to search for neutrinos coincident with GRBs with short latency and contribute to the Gamma-ray Coordinate Network (GCN) by submitting notices when candidate events are detected [3]. The mechanism for such alerts is outlined in section 8.

2. IceCube

IceCube is a cubic kilometer scale ice Cherenkov detector instrumented in the polar ice cap at the South Pole. The full detector, completed in December of 2010, consists of 5160 optical modules (DOMs) deployed along 86 vertical strings. The active volume begins about 1.5 km below the surface to shield low energy cosmic ray muons. High-energy charged leptons produce Cherenkov radiation as they propagate through the ice. This radiation may be detected by the DOMs, each of which contains a 10-inch photomultiplier tube that converts the collected radiation into an amplified analog pulse that is subsequently digitized on board and sent to the data acquisition (DAQ) system on the surface where the trigger conditions are applied. The triggered events are then processed and filtered at the South Pole. A number of fast reconstructions are applied to the events before the data are saved and transferred to the north via a TDRSS satellite link.

3. Event Reconstructions

Triggered events passing simple event classification filters are reconstructed online using a maximum likelihood method [4]. The reconstruction fits the temporal and spatial topologies of the DOMs that detected a signal in each event. For this analysis, only upward going muon track events are considered for which a neutrino pure signal is attainable due to the Earth’s shielding of cosmic ray muons. The region beyond the horizon, down to a declination of -5° , is also included because the ice cap is thick enough in this region to provide sufficient overburden.

The parameters used for event selection are described in section 4. Of primary importance to the analysis are the energy and angular reconstructions. From simulation we have determined that the angular resolution on track events is better than 1° for energies greater than 3 TeV. At the energies that IceCube is sensitive to, the relativistic boost factor is large and the neutrino and muon are highly collinear, such that the reconstructed muon vector can be used to point back in the direction of the incoming neutrino. An estimate of the reconstructed energy may be obtained by measuring the total charge deposited to all DOMs during an event. This energy estimate can only provide a lower bound on the true neutrino energy since a portion of the incoming and/or outgoing track is typically not contained. Assuming an E^{-2} spectrum, the median energy error is a factor of 4 times the reconstructed energy. Nevertheless, the steeply falling energy distribution of the background flux renders the energy estimate useful for distinguishing background from signal.

4. Event Selection

Despite searching for upward going neutrinos, the dominant background at trigger level is due to downward going cosmic ray muons which trigger IceCube at a rate of about 2.5 kHz. Most of these muons will be properly reconstructed as downward going and removed from the analysis, but some downward going muons are mis-reconstructed as upward going. Muons passing near the boundary of the instrumented volume can produce light patterns that propagate upwards, and coincident cosmic ray muons can also leave light patterns that reconstruct as upward going. Both cases are well distinguished from true upward going muons using fit quality, fit stability, and event topology parameters. After loose pre-cuts that mostly remove poorly reconstructed events, 13 parameters are used to train Boosted Decision Tree forests using well reconstructed simulated neutrinos as signal and off-time (not within ± 2 hours of a GRB) data as background.

An irreducible background of atmospheric neutrinos will remain in the sample at final cut level. On time atmospheric neutrinos are indistinguishable from neutrinos produced by GRBs, and can only be probabilistically differentiated based on their energy and direction with respect to a known GRB. The final cut level is optimized for discovery potential independently for each detector configuration. At this level, well reconstructed simulated neutrinos following an E^{-2} spectrum have a greater than 80% efficiency with respect to trigger level, and yield a final event rate of less than 4 mHz.

5. GRB Selection

Notices and circulars reported to the GRB Coordinates Network (GCN) [3] by satellite experiments are parsed and stored by an automated system called GRBWeb [5]. GRBWeb is available on

the web and provides per burst information from the experiments reporting GRB detection. When multiple satellites observe the same burst, the time window is defined by the most inclusive start and stop times reported. The angular position and error is given by the satellite with the smallest reported angular error, and the spectral parameters of the gamma ray fluence are preferentially taken from Fermi GBM [6] [7], Konus-Wind [8], Suzaku [9], Swift/BAT [10], and INTEGRAL [11], in that order. The gamma ray fluence parameters are used for modeling the neutrino fluence predictions. When a parameter is not reported, an average value is used, where the average values are calculated separately for short bursts (less than 2 s) and long bursts (greater than 2 s).

6. Analysis

The analysis presented here is designed to discover a neutrino signal arriving from the direction of a known GRB coincident in time with the gamma ray signal observed by a satellite experiment. Neutrino emission models that do not adhere to this paradigm are not well constrained by such an analysis. To determine the level at which the observed data supports the hypothesis that GRBs produce neutrinos, an unbinned likelihood analysis is used. The underlying likelihood function is a ratio of signal like to background like probability density functions (PDFs) that describe the relative probabilities of observing a signal or background event as a function of reconstructed event energy, event time with respect to the observed gamma ray emission time, and the event direction with respect to the observed GRB location. It is denoted as $S/B = (S/B)_{\text{energy}} \times (S/B)_{\text{time}} \times (S/B)_{\text{space}}$.

To calculate the $(S/B)_{\text{energy}}$ term, the reconstructed energies of simulated neutrino events, weighted to an E^{-2} spectrum, are used to describe the signal PDF. The background energy PDF is taken from off-time data. Beyond 100 TeV, the low number of observed data events start to add statistical uncertainty to the PDF ratio. To remove the effects of this uncertainty at high energy, the simulated neutrino sample is weighted to an atmospheric neutrino flux model and used to extend the background energy PDF beyond 10 PeV.

The $(S/B)_{\text{time}}$ term is calculated based on the time difference between the observed event time and the GRB start time, $\Delta t = (t_{\text{event}} - t_{\text{GRB}})$. The signal time PDF is constructed to have constant probability during the gamma detection duration. Gaussian tails are appended prior to the start, and following the end of the burst duration. The width of the appended Gaussian functions is given by the burst duration, where a minimum of 2 s and maximum of 30 s is imposed if the burst duration is outside of this range. This treatment preserves some sensitivity to precursor and afterglow periods. The Gaussians are normalized such that there is a smooth transition at the boundaries of the burst start and end times. To lower processing time, the tails of the signal time PDF are truncated at four times the width (4σ) so that events outside this window automatically receive a signal PDF equal to zero, and therefore need not be considered. A constant value is used for the background time PDF and is defined over the same interval for which the signal time PDF is non-zero.

Finally, the term $(S/B)_{\text{space}}$ is constructed from $\Delta\Psi$, the opening angle between the reconstructed event direction and observed GRB direction vectors, along with the associated errors on those directions. A recent modification to the analysis is the use of the Kent distribution [12], a probability density function normalized on the unit sphere which provides a better description to the spread in angular directions than the previously used circularized two dimensional Gaussian. Assuming circularized errors, such that the contours of equal probability on the sphere are circular,

the Kent distribution simplifies to $f(\Delta\Phi, \kappa) = (\kappa/4\pi\sinh(\kappa)) \times \exp(\kappa\cos(\Delta\Phi))$, where κ sets the spread of the distribution and is taken to be $\kappa = 1/(\sigma_{\text{GRB}}^2 + \sigma_{\text{event}}^2)$. This new treatment has a very small impact on the muon track analysis because the event and GRB angular errors are typically well below about 20° when the difference between the Kent and Gaussian treatments becomes noticeable in the tails. For consistency, however, this treatment was adopted because it is necessary for complementary analyses that accept cascade like events from ν_e and ν_τ charged current interactions as well as neutral current interactions. These events typically have poor pointing resolution, often greater than 20° . The background space PDF is determined from off-time data and accounts for the geometrical efficiencies of the detector from various directions.

For an ensemble of events, the PDFs can be used to evaluate how signal or background like the events are. The following test statistic is used to encapsulate the degree to which an ensemble of N events is signal like or background like:

$$T = -n_s + \sum_{i=1}^N \ln \left(\frac{n_s S_i}{\langle n_b \rangle B_i} + 1 \right),$$

which is the logarithm of the likelihood that the ensemble represents $n_s + \langle n_b \rangle$ signal plus background events, divided by the likelihood that the ensemble represents only $\langle n_b \rangle$ background events and no signal events. The value of n_s is chosen such that it maximizes this log likelihood ratio for the given event ensemble. So far, IceCube has yet to observe a statistically significant neutrino event on time and on source with a GRB, and so limits are placed on various neutrino production models. The best limits are derived by "stacking" the GRB time windows into one single exposure. The value of $\langle n_b \rangle$ is then determined for the entire exposure under consideration. In the future, we will also evaluate T over the time window of each GRB. For such per GRB test statistics, the value of $\langle n_b \rangle$ is much smaller due to the smaller time window.

The significance of an observed T value, T_{obs} , is obtained from a comparison against the distribution of T assuming that only background events are present. For many trials, pseudo events are selected based on the background energy and space PDFs from the off-time data. Arbitrary signal models can be tested by injecting not only background events, but also signal like events from simulation which are drawn according to the signal energy, space, and time PDFs, where each event carries a weight determined by the specific signal model under consideration. The weight for each signal event is equivalent to the probability that such an event should be injected. For a given signal model, the signal strength is adjusted while evaluating a sufficiently large number of random trials. Following the Feldman-Cousins prescription [13], a 90% confidence upper limit is determined by the signal strength required such that 90% of trials yield a T greater than T_{obs} .

7. Recent Results

The latest results from IceCube are based on the analysis of four years of data, three years while under construction and one year with the completed detector, and no significant correlation between known GRBs and upward going neutrino events was found [14]. A single event was found that correlates to an observed GRB, however, even though the event was on time, it was not within the 1σ angular error circle, and had a relatively modest muon reconstructed energy of 10 TeV. Combining all of the GRBs into a single stacked exposure yields a test statistic, $T = 0.1330$ which

corresponds to a significance of $p = 0.33$. In lieu of a signal discovery, these results can be used to improve the limits on various GRB neutrino production models. A general class of models exists where neutrinos are produced via $p\gamma$ interactions in a GRB fireball. Assuming that GRBs are the dominant sources of cosmic rays observed at Earth, these models predict a doubly-broken power law spectrum in the Earth's frame. This total quasi-diffuse flux is given by:

$$\Phi_\nu(E) = \Phi_0 \cdot \begin{cases} E^{-1} \epsilon_b^{-1} & E < \epsilon_b, \\ E^{-2} & \epsilon_b \leq E < 10\epsilon_b, \\ E^{-4} (10\epsilon_b)^2 & 10\epsilon_b \leq E. \end{cases}$$

Exclusion contours are shown in Figure 1. Also shown on the plot are two representative model predictions assuming prompt neutrino emission. The first assumes that only neutrons escape from the GRB fireball to contribute to the UHECRs [15]. This scenario predicts a large neutrino flux, and is strongly excluded by the limits. The second prediction, the Waxman-Bahcall model, allows for direct proton escape from the GRB fireball and hence can account for the UHECRs without requiring a large neutrino flux [16]. We do not yet fully exclude this scenario at the 90% confidence level. More details on the results are available in reference [14].

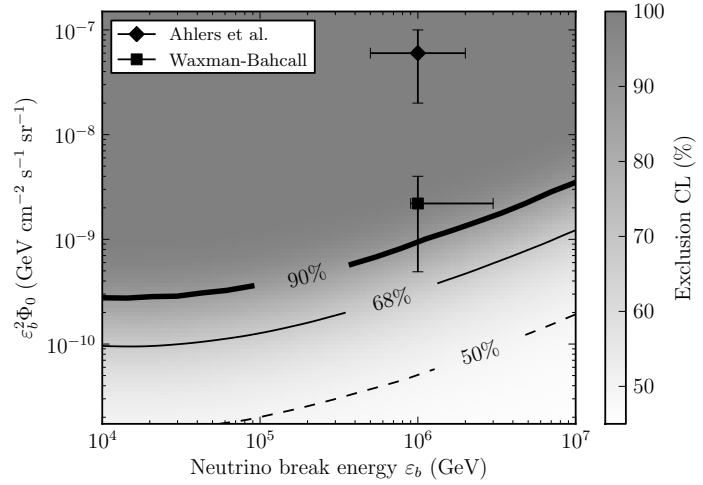


Figure 1: Exclusion regions for a generic double broken power law ν flux models as a function of the spectrum break energy, ϵ_b , and flux normalization, Φ_0 .

8. Near Realtime Alerts

In view of the recent results, the current limits already place tight constraints on typical model assumptions for prompt neutrino production in GRBs. In the near future, data from three additional years taken with the completed IceCube detector will be included and searches for cascade like events as well as muon tracks originating from the southern sky will be considered. Whether a signal is present or not, we wish to maximize our chances for a discovery. In pursuit of this goal, a near realtime data processing system has been created to allow IceCube to further contribute to the multi-messenger strategy for studying GRBs.

Due to the logistical challenges of working from the South Pole, a processing pipeline has been developed in the north to process IceCube data as quickly as possible. Although computer resources are abundant outside of the South Pole, a significant delay is suffered due to the existing data transfer procedures which rely on a transfer link via TDRSS satellite. Data taken by IceCube is typically not available elsewhere for at least about one day after the data was taken. Once the data is available, the processing pipeline is very fast and adds minimally to the total latency. Figure

2 shows the observed latency of this system for the time period just prior to submitting these proceedings. It is evident that the typical latency of this system is between one and two days, as expected.

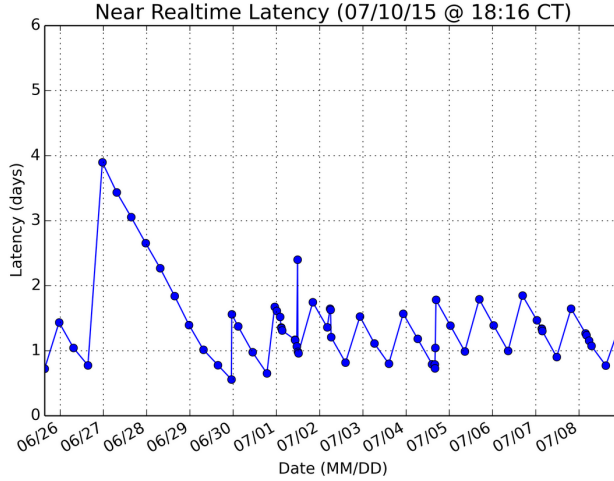


Figure 2: Observed latency of IceCube data with the northern track GRB event selection applied. The Latency is dominated by delay of daily TDRSS transfer link and is typically in the range of one to two days; occasionally it will increase for a few days.

is observed. Such a mechanism is under development, but it is expected that the northern track analysis will be the first implemented by this system.

The analysis of events will follow the per-burst description provided in Section 6. The standard signal and background PDFs will be used to evaluate the test statistic only including the time window when the signal time PDF is non-zero. The significance for a single coincident event will be larger in the per-burst case because the average expected background rate is suppressed by the short search duration. The per-burst calculation is also more sensitive to multiplet signals where two or more events are seen on time with a GRB. A single high-energy on time on source event, or two events with modest energy, could very well constitute a discovery.

If the per-burst analysis returns a zero test statistic, no alert is generated. If a non-zero test statistic is returned, an automated alert will be generated and submitted to GCN as a notice. If further information is either needed or available, the notice will be followed up by a circular that details the event(s) contributing to the alert. There is also a desire to archive a subset of the neutrino events with the Astrophysical Multimessenger Observatory Network (AMON) for use in additional correlation studies of a possible simultaneous detection of sub discovery threshold events among two or more contributing observatories [17].

For the northern track analysis, all necessary reconstruction variables are immediately available as they are calculated online at the South Pole. Events which pass the event selection are stored locally and compared to a running GRB sample compiled from GRBweb every 10 minutes. In some cases, the GRB information may lag behind the neutrino data. Therefore, the analysis is triggered both when new events are processed, and when new GRB information is available. For future southern track and cascade analyses, the event selection requires additional computation time that makes it unfeasible to select events in realtime. The possibility does exist, however, to trigger such searches when a new GRB

9. Conclusion

IceCube has searched for upward going muon neutrinos in coincidence with GRBs detected by satellite observatories. So far no significant detection has been made and the absence of a signal is used to place strong limits on models predicting prompt neutrino production in GRB fireballs. Many additional models exist which are not explicitly tested by current analyses. A web based tool was developed for public use that allows anyone to derive limits to their chosen model based on the four year IceCube northern track search. The link is available in reference [18]. As IceCube continues, a near realtime (latency of one to two days) data processing and alert system will soon be implemented to quickly search for a coincident neutrino signal from newly observed GRBs. If a detection is made, we wish to alert the community to allow for follow up observations by satellite and ground based observatories.

References

- [1] E. Waxman, *Phys. Rev. Lett.* **75** (1995) 386 [astro-ph/9505082].
- [2] M. G. Aartsen, et al., *Science* **342** (2013) 1242856 [arXiv:1311.5238].
- [3] The Gamma-ray Coordinates Network. <http://gcn.gsfc.nasa.gov/>
- [4] J. Ahrens, et al., *Nucl. Instrum. and Meth. A* **524** (2004) 169 [astro-ph/0407044].
- [5] GRBweb. <http://grbweb.icecube.wisc.edu/>
- [6] W. Paciesas, et al., *ApJS* **199** (2012) 18 [arXiv:1201.3099].
- [7] A. Goldstein, et al., *ApJS* **199** (2012) 19 [arXiv:1201.2981].
- [8] R. Aptekar, et al., *Space Sci. Rev.* **71** (1995) 265.
- [9] K. Yamaoka, et al., *Publ. Astron. Soc. Japan* **61** (2009) 1117 [arXiv:0906.3515].
- [10] N. Gehrels, et al., *ApJ* **611** (2004) 1005 [astro-ph/0405233].
- [11] C. Winkler, et al., *Astron. Astrophys.* **411** (2003) L1.
- [12] J. Kent, *Journal of the Royal Statistical Society B* **44** (1982) 71.
- [13] G. Feldman, R. Cousins, *Phys. Rev. D* **57** (1998) 3873 [physics/9711021].
- [14] M. G. Aartsen, et al., *ApJ* **805** (2015) L5 [arXiv:1412.6510].
- [15] M. Ahlers, et al., *Astroparticle Physics* **35** (2011) 87 [arXiv:1103.3421].
- [16] E. Waxman, J. Bahcall, *Phys. Rev. Lett.* **78** (1997) 2292 [astro-ph/9701231].
- [17] M. W. E. Smith, et al., *Astroparticle Physics* **45** (2013) 56 [arXiv:1211.5602].
- [18] IceCube GRB Limit Tool. <http://icecube.wisc.edu/science/tools/grblimits>

Search for neutrino emission from extended sources with the IceCube detector

The IceCube Collaboration¹,

¹ http://icecube.wisc.edu/collaboration/authors/icrc15_icecube

E-mail: epinat@icecube.wisc.edu

The IceCube Neutrino Observatory, a cubic kilometer telescope located in the Antarctic ice, offers unique opportunities to study high-energy neutrino emission from galactic and extragalactic sources. The Galactic plane is the brightest source of gamma rays in the sky, and it is believed to be also one of the brightest sources of very energetic neutrinos. The first discovery of an astrophysical high-energy neutrino flux has recently been announced by the IceCube collaboration and, although no clear sources have been found so far, it is reasonable to investigate whether a Galactic component might be contributing to the observed flux. As indicated by the HESS gamma-ray survey and by Milagro as well, many of the sources populating the Galactic plane are in fact extended sources. The sensitivity and discovery potential of IceCube for neutrinos coming from extended regions using 6 years of data are being presented in this contribution.

Corresponding authors: Elisa Pinat^{*†}, Juan Antonio Aguilar Sánchez[†],

[†] *Université Libre de Bruxelles,*

Interuniversity Institute for High Energies (IIHE), 1050 Brussels, Belgium

*The 34th International Cosmic Ray Conference,
30 July- 6 August, 2015
The Hague, The Netherlands*

^{*}Speaker.

1. Introduction

IceCube is a cubic kilometer neutrino detector installed in the ice at the geographic South Pole between depths of 1450 m and 2450 m [1]. Detector construction started in 2005 and finished in 2010. During the construction period, IceCube collected data in four different configurations, until the final 86 string one was achieved starting from 2011. Neutrino reconstruction relies on the optical detection of Cherenkov radiation emitted by secondary particles produced in neutrino interactions in the surrounding ice or the nearby bedrock. Neutrinos have unique properties that can be used to probe various astrophysical processes. Produced in the same environment as Cosmic Rays (CRs) and Gamma Rays, their neutral charge allows them to travel straight from the source to Earth, preserving directional information. Furthermore, the fact that they only interact weakly allows them to travel large distances without being hindered by intervening matter. Astrophysical neutrinos are also tracers of hadronic interactions, and the identification of these neutrino sources may help to clarify cosmic ray acceleration processes. The recent discovery by IceCube of a diffuse high-energy astrophysical neutrino flux [2][3] is now established at a 7σ confidence level [4], but no sources have been identified yet. Finding neutrino sources in the sky requires locating an excess of events from a particular direction over the background of atmospheric neutrinos and muons. The energy distribution of events is used as discriminator between the signal and the background hypotheses [5]. In these proceedings we focus on spatially extended sources: many have been already identified in the gamma sky and if a neutrino counterpart is found they will help unravel the mysteries of cosmic ray acceleration. Sensitivities and discovery potential will be shown on data from three years of operation in partial levels of completion (IC-40, IC-59 and IC-79) and the first three years of the completed 86 string detector (IC86-I, IC86-II, IC86-III). The previous extended source analysis was limited to the data of the first IC86-I sample, and the results are shown in [6].

2. Scientific motivation

The Galactic plane is the brightest source of γ -rays in the sky [7][8]. Among other processes, the γ -ray emission from the Galaxy originates also from the cosmic ray interaction in the interstellar medium. In these interactions, the production of neutral and charged pions, and their subsequent decay, results into γ -ray, electron/positron and neutrino emission. The HESS survey of the inner part of the Galactic Plane [9] has revealed a number of bright extended γ -ray sources and it is thus the γ -ray astronomy that provides a strong motivation to look for extended sources. The same sources are also seen in the survey of the Galactic Plane above 100 GeV performed by Fermi-LAT [10], and it is possible that these are also the locations of recent injections of $E > 1$ TeV cosmic rays in the Galaxy [10]. If the observed γ -rays are produced by CR interactions, a very-high-energy neutrino flux should be associated as well. If detected, this would represent an unambiguous proof of the hadronic nature of the sources.

Motivation in favour of a dedicated extended source analysis is also obtained from Fig. 1. Assuming the presence of extended sources and modelling the signal injection accordingly to its extension, this plot shows the comparison between an analysis that uses the regular point source method to analyse this signal and an analysis that instead takes into account the spatial extension

in the likelihood method, assuming each time a different spatial extension from 1° to 5° [6]. The median angular resolution of the detector varies with energy, but for well reconstructed tracks can be $< 1^\circ$. The discovery potential for an E^{-2} flux of the regular point source analysis method is compared to the one calculated with our extended source analysis. In this case, the same value used to simulate the spatial extension enters the likelihood calculation, showing that, when the correct source extension is used, the improvement is noticeable. Since the source extension is not known a priori, several assumptions will be made, from one to five degrees.

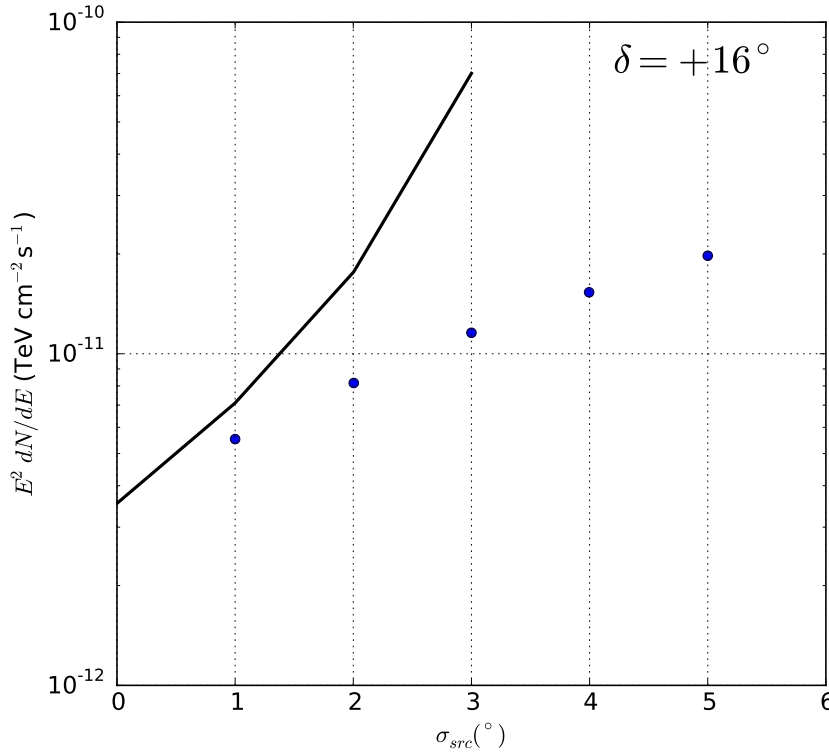


Figure 1: Discovery potential for an E^{-2} flux from an extended source at a declination of 16° for one year of IC86 data with no trial factor correction. The regular point source analysis (solid-line) is compared to the discovery potential of the extended source analysis using always the correct source extension (blue dots).

3. Analysis method

This analysis uses an unbinned maximum likelihood test [11], that allows to calculate the significance of an excess of neutrinos above the background for a given direction. Both the reconstructed direction of the event and the reconstructed deposited muon energy are used to discriminate between signal and background. Since signal events have a harder energy spectrum compared to

the atmospheric neutrino and muon background [12], this method performs better than a simple directional clustering approach [13]. The signal and background probability density functions (p.d.f.) are a function of the reconstructed declination and the reconstructed muon energy. For a data sample of N total events, the p.d.f. of the i^{th} event in the j^{th} sample (IC40, IC59, IC79, IC86-I, IC86-II or IC86-III) with reconstructed energy E_i and angular distance to the source $|\vec{x}_i - \vec{x}_s|$ is given by:

$$P_i^j(|\vec{x}_i - \vec{x}_s|, E_i, \gamma, n_s^j) = \frac{n_s^j}{N^j} S_i^j + \left(1 - \frac{n_s^j}{N^j}\right) B_i^j$$

where S_i^j and B_i^j are the signal and background p.d.f. respectively, and n_s^j is the number of signal events expected from the corresponding j^{th} sample. The signal p.d.f. used is given by:

$$S_i^j = s_i^j(|\vec{x}_i - \vec{x}_s|, \sigma_i, \sigma_{src}) \varepsilon_i^j(E_i, \delta_i, \gamma)$$

here s_i^j is the space contribution and depends on the angular uncertainty of the event, σ_i , the angular difference between the reconstructed direction of the event and the source position and the extension of the source. The spatial probability distribution function is still assumed to be a 2-D Gaussian but, contrary to the regular point source analysis, the width is determined by:

$$S_i = \frac{1}{2\pi(\sigma_i^2 + \sigma_{src}^2)} \exp\left(-\frac{|\vec{x}_i - \vec{x}_s|^2}{2(\sigma_i^2 + \sigma_{src}^2)}\right)$$

The energy ε_i^j and background B_i^j p.d.f remain the same as for the regular point source method described in Ref. [3]. The simulation of an extended source is performed by sampling events from several injected point sources distributed according to the source extension. To parametrize the extended source we use the Kent distribution [14], which for small values of sigma ($< 8^\circ$) can roughly be considered as a Gaussian normalized on a sphere. The signal injection simulation is used for sensitivity and discovery potential calculations, but also to calculate the relative efficiencies of the different detector geometries when combining several years of data.

The likelihood is a function of two fit parameters: n_s , the number of signal events originating from the source, and γ , the spectral index of a neutrino source with a power law spectrum, which are maximized for a given location in the sky. The significance is then estimated using the log-likelihood ratio as the test statistic as described in Ref. [11]. This proposed analysis is expanded to several years of different detector geometries as described in Ref. [15].

4. Performance

In this section we show the performance of an all-sky scan searching for sources of 1° , 2° , 3° , 4° and 5° extension as a function of declination. Figure 2 shows the sensitivity for a ν_μ flux at the 90% C.L. whereas Fig.3 shows the discovery potential. The silver band represents the coverage from 1° to 5° source extension for six years of data, whereas the black lines are relative to the previous 4 years analysis, the solid line for 1° extension and the dotted one for 5° . For comparison, the four years regular point source analysis reports, for an E^{-2} spectrum, a median sensitivity value at 90% C.L. of $\sim 10^{-12} \text{ TeV}^{-1} \text{ cm}^{-2} \text{ s}^{-1}$ for energies between 1 TeV-1 PeV in the northern sky and of $\sim 10^{-11} \text{ TeV}^{-1} \text{ cm}^{-2} \text{ s}^{-1}$ for energies between 100 TeV-100 PeV in the southern sky [6]. For the

moment, six years of data have been simulated by adding two more times the dataset relative to IC86-I. These datasets are the ones that have been used for point source searches, where the background rejection is optimised for better angular resolution. For this reason, sensitivity studies will be performed to determine instead how to optimize the event selection for extended sources.

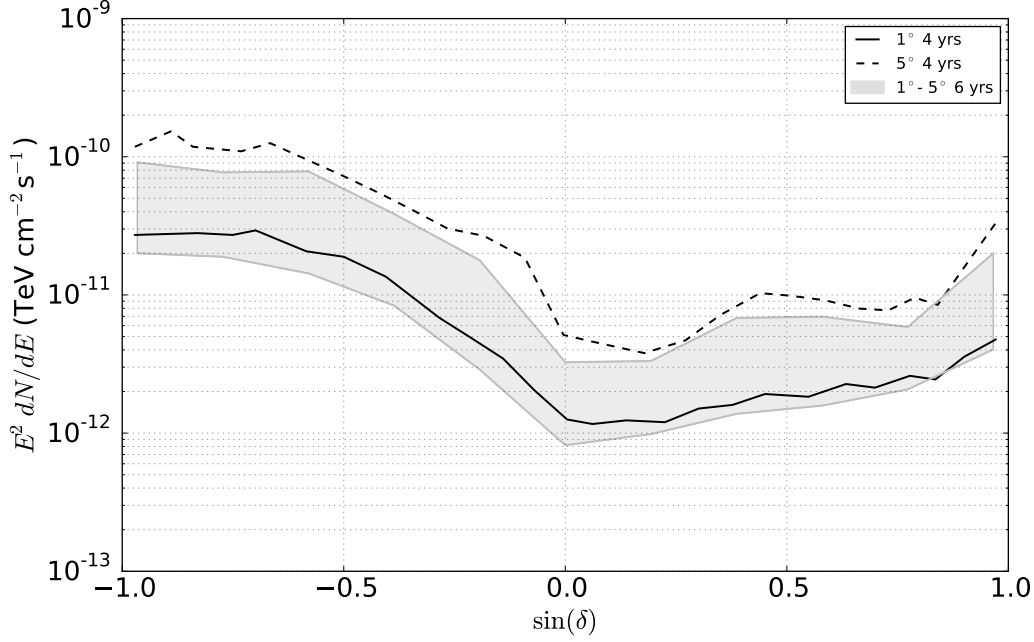


Figure 2: Sensitivity for an E^{-2} neutrino flux from an extended source considering various extensions from one to five degrees, using the correct extension in the likelihood. The silver band represent the 6 years sensitivity interval from 1° to 5° source extension, whereas the black solid and dotted lines represent the sensitivity for 1° and 5° for 4 years of data.

5. Conclusions and Outlook

The goal of this analysis is to produce a set of significance skymaps for various source extensions. For each extension scan, the highest significant coordinate will be selected and the most significant location of the various maps will be used to determine the final p-value. The trial factor arising from the all-sky scan of each search will be taken into account by generating average background samples using the right ascension scrambling technique in order to estimate how often the background can produce a p-value as significant as the one observed [5]. The trial factor among the various skymaps will be conservatively assumed to be just the number of produced maps.

Although not as sensitive as regular point source searches for point-like sources, extended searches investigate a different signal hypothesis where the no-extension assumption is strongly penalized if the neutrino source has truly an extension. Many astrophysical surveys have already

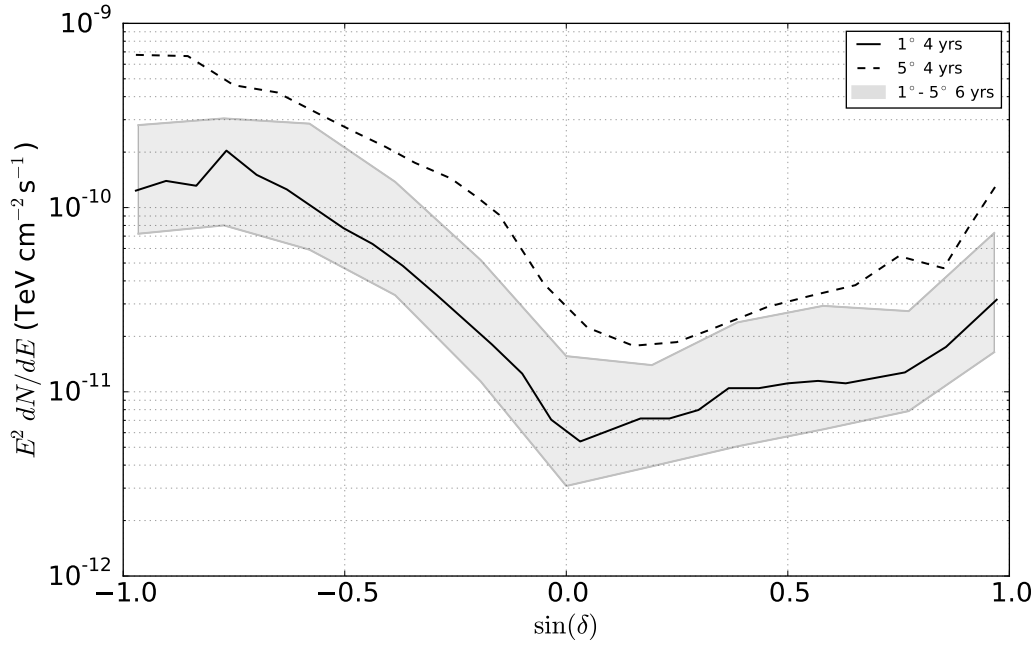


Figure 3: Discovery potential for an E^{-2} neutrino flux from an extended source considering various extensions from one to five degrees, using the correct extension in the likelihood. The silver band represent the 6 years discovery potential interval from 1° to 5° source extension, whereas the black solid and dotted lines represent the discovery potential for 1° and 5° for 4 years of data.

revealed the presence of extended sources in the gamma sky, but the identification of a neutrino counterpart is still a challenge. If found, however, it would help reveal the sources and underlying physics processes of cosmic ray acceleration.

References

- [1] **IceCube** Collaboration, A. Achterberg et al., *Astroparticle Physics* **26** (2006) 155–173, [[astro-ph/0604450](#)].
- [2] **IceCube** Collaboration, M. Aartsen et al., *Science* **342** (2013) 1242856, [[arXiv:1311.5238](#)].
- [3] **IceCube** Collaboration, M. Aartsen et al., *Phys.Rev.Lett.* **113** (2014) 101101, [[arXiv:1405.5303](#)].
- [4] **IceCube** Collaboration, *PoS(ICRC2015)1081*, these proceedings.
- [5] J. Braun, J. Dumm, F. De Palma, C. Finley, A. Karle, et al., *Astroparticle Physics* **29** (2008) 299–305, [[arXiv:0801.1604](#)].
- [6] **IceCube** Collaboration, M. Aartsen et al., [arXiv:1406.6757](#).
- [7] W. L. Kraushaar, G. W. Clark, G. P. Garmire, R. Borken, P. Higbie, V. Leong, and T. Thorsos, *The Astrophysical Journal* **177** (Nov., 1972) 341.
- [8] M. Ackermann et al., *The Astrophysical Journal* **750** (May, 2012) 3, [[arXiv:1202.4039](#)].
- [9] F. Aharonian et al., *Astronomy and Astrophysics* **477** (Jan., 2008) 353–363, [[arXiv:0712.1173](#)].
- [10] A. Neronov and D. V. Semikoz, *Phys. Rev. D* **85** (Apr, 2012) 083008.
- [11] J. Braun, M. Baker, J. Dumm, C. Finley, A. Karle, and T. Montaruli, *Astroparticle Physics* **33** (Apr., 2010) 175–181, [[arXiv:0912.1572](#)].
- [12] **IceCube** Collaboration, M. Aartsen et al., *Phys.Rev.* **D91** (2015), no. 2 022001, [[arXiv:1410.1749](#)].
- [13] **IceCube** Collaboration, R. Abbasi et al., *The Astrophysical Journal* **732** (2011), no. 1 18.
- [14] J. T. Kent, *Journal of the Royal Statistical Society. Series B (Methodological)* (1982) 71–80.
- [15] **IceCube** Collaboration, M. Aartsen et al., *The Astrophysical Journal* **779** (2013), no. 2 132.

